พลวัตเชิงโมเลกุลของท่อนาโนคาร์บอนชั้นเดียวที่พันรอบด้วยพอลิโพรพิลีน
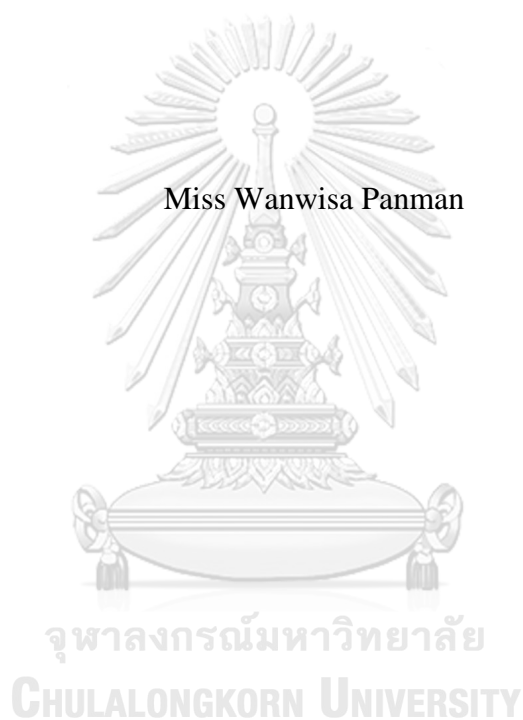
นางสาววันวิสาข์ ปานมั่น

วิทยานิพนธ์นี้เป็นส่วนหนึ่งของการศึกษาตามหลักสูตรปริญญาวิทยาศาสตรมหาบัณฑิต
สาขาวิชาปิโตรเคมีและวิทยาศาสตร์พอลิเมอร์
คณะวิทยาศาสตร์ จุฬาลงกรณ์มหาวิทยาลัย
ปีการศึกษา 2560
ลิขสิทธิ์ของจุฬาลงกรณ์มหาวิทยาลัย

MOLECULAR DYNAMICS OF SINGLE-
WALL CARBON NANOTUBE WRAPPED WITH POLYPROPYLENE

Miss Wanwisa Panman

A Thesis Submitted in Partial Fulfillment of the Requirements
for the Degree of Master of Science Program in Petrochemistry and Polymer Science
Faculty of Science
Chulalongkorn University
Academic Year 2017
Copyright of Chulalongkorn University

Thesis Title	MOLECULAR DYNAMICS OF SINGLE-WALL CARBON NANOTUBE WRAPPED WITH POLYPROPYLENE
By	Miss Wanwisa Panman
Field of Study	Petrochemistry and Polymer Science
Thesis Advisor	Professor Supot Hannongbua, Dr.rer.nat.
Thesis Co-Advisor	Assistant Professor Thanyada Rungrotmongkol, Ph.D.
	Oraphan Saengsawang, Dr.rer.nat.

Accepted by the Faculty of Science, Chulalongkorn University in Partial Fulfillment of the Requirements for the Master's Degree

.... Dean of the Faculty of Science
(Associate Professor Polkit Sangvanich, Ph.D.)

THESIS COMMITTEE

.... Chairman
(Professor Suda Kiatkamjornwong, Ph.D.)

.... Thesis Advisor
(Professor Supot Hannongbua, Dr.rer.nat.)

.... Thesis Co-Advisor
(Assistant Professor Thanyada Rungrotmongkol, Ph.D.)

.... Thesis Co-Advisor
(Oraphan Saengsawang, Dr.rer.nat.)

.... Examiner
(Assistant Professor Rojrit Rojanathanes, Ph.D.)

.... External Examiner
(Chompoonut Rungnim, Ph.D.)

วันวิสาข์ ปานมั่น : พลวัตเชิงโมเลกุลของท่อนาโนคาร์บอนชั้นเดียวที่พันรอบด้วยพอลิ โพรพิลีน (MOLECULAR DYNAMICS OF SINGLE-WALL CARBON NANOTUBE WRAPPED WITH POLYPROPYLENE) อ.ที่ปรึกษาวิทยานิพนธ์ หลัก: ศ. ดร.สุพจน์ หารหนองบัว, อ.ที่ปรึกษาวิทยานิพนธ์ร่วม: ผศ. ดร.ธัญญดา รุ่งโรจน์ มงคล, ดร.อรพรรณ แสงสว่าง, 42 หน้า.

ปัจจุบันวัสดุนาโนคอมพอสิตได้รับความนิยมอย่างแพร่หลายในหลาย ๆ การใช้งาน เนื่องจากมีสมบัติเด่นด้านการนำความร้อนและนำไฟฟ้าได้ดี วัสดุนาโนคอมพอสิตที่เกิดจากการ ผสมกันระหว่างพอลิเมอร์กับท่อนาโนคาร์บอน คือวัสดุนาโนคอมพอสิตชนิดหนึ่งที่ได้รับความ สนใจ และที่ผลิตขึ้นเพื่อปรับปรุงการนำความร้อนและสมบัติทางไฟฟ้าของพอลิเมอร์ แต่อย่างไรก็ ตาม วัสดุนาโนคอมพอสิตที่ผสมกันระหว่างพอลิโพรพิลีนกับท่อนาโนคาร์บอนก็ประสบปัญหาใน การสังเคราะห์ เนื่องจากการผสมท่อนาโนคาร์บอนและพอลิโพรพิลีนเข้ากันได้ไม่ดี ซึ่งเป็นผลมา จากการรวมตัวกันเป็นกลุ่มก้อนของท่อนาโนคาร์บอน ดังนั้นงานวิจัยนี้จึงเลือกอะไมโลส และไค โทซานซึ่งเป็นพอลิเมอร์ชีวภาพมาใช้ในการแก้ปัญหาดังกล่าว โดยการนำเลือกอะไมโลส และไค โทซานมาพันรอบท่อนาโนคาร์บอนชั้นเดียว เพื่อปรับปรุงพื้นผิวของท่อนาโนคาร์บอนชั้นเดียวด้วย การจำลองพลวัตเชิงโมเลกุล จากผลการจำลองพลวัตเชิงโมเลกุล พบว่าอะไมโลส และไคโทซาน สามารถเหนี่ยวนำให้พอลิโพรพิลีนทั้ง 3 ชนิดคือ อะแทกติก ไอโซแทกติก และซินดิโอแทกติกพอ ลิโพรพิลีนพันรอบท่อนาโนคาร์บอนได้ดีขึ้น ซึ่งพอลิเมอร์ชีวภาพทั้ง 2 ชนิดมีความสามารถในการ เหนี่ยวนำให้พอลิโพรพิลีนพันรอบท่อนาโนคาร์บอนในลักษณะที่ต่างกัน คือ อะไมโมสเหนี่ยวนำ ให้พอลิโพรพิลีนพันรอบท่อนาโนคาร์บอนในลักษณะบิดเป็นเกลียวและสัมผัสกับผิวท่อนาโน คาร์บอนโดยตรง จากการพันรอบท่อนาโนคาร์บอนในลักษณะเกลียวนี้ทำให้ค่ารัศมีไจเรชันของพอ ลิโพรพิลีนมีค่าลดต่ำลงและต่ำกว่าค่าจากอะไมโลส ส่วนไคโทซานเหนี่ยวนำให้พอลิโพรพิลีนพัน รอบท่อนาโนคาร์บอนในลักษณะคล้ายงูเลื้อยโดยเกิดอันตรกิริยากับผิวด้านนอกของไคโทซาน และ มีค่ารัศมีไจเรชันของพอลิโพรพิลีนมีค่าไม่เปลี่ยนแปลงมากนักแต่สูงกว่าค่าจากอะไมโลส โดย พบว่าอันตรกิริยาที่สำคัญที่เหนี่ยวนำให้พอลิโพรพิลีนพันรอบท่อนาโนคาร์บอนได้ดี คือ อันตร กิริยาแบบไฟฟ้าสถิต

สาขาวิชา	ปิโตรเคมีและวิทยาศาสตร์พอลิเมอร์	ลายมือชื่อนิสิต
ปีการศึกษา	2560	ลายมือชื่อ อ.ที่ปรึกษาหลัก
		ลายมือชื่อ อ.ที่ปรึกษาร่วม
		ลายมือชื่อ อ.ที่ปรึกษาร่วม

5872147623 : MAJOR PETROCHEMISTRY AND POLYMER SCIENCE

KEYWORDS: NANOCOMPOSITE MATERIALS, CARBON NANOTUBE, AMYLOSE, CHITOSAN, POLYPROPYLENES, MOLECULAR DYNAMICS SIMULATION

WANWISA PANMAN: MOLECULAR DYNAMICS OF SINGLE-WALL CARBON NANOTUBE WRAPPED WITH POLYPROPYLENE. ADVISOR: PROF. SUPOT HANNONGBUA, Dr.rer.nat., CO-ADVISOR: ASST. PROF. THANYADA RUNGROTMONGKOL, Ph.D., ORAPHAN SAENGSAWANG, Dr.rer.nat., 42 pp.

Nowadays, the nanocomposite materials have been widely used in various applications due to their unique properties such as thermal and electrical properties. Polymer/carbon nanotube (CNT) nanocomposite is one the important nanocomposite materials that are manufactured for improving thermal conductivity and electrical properties of polymers. Unfortunately, polypropylene (PP)/CNT preparation is difficult because of CNT dispersion and aggregation. Accordingly, amylose (AMY) and chitosan (CS) are selected in the present study in order to demonstrate how AMY and CS could diminish such problems by non-covalent modification on outer surface of single-walled CNT using molecular dynamics (MD) simulations. The MD results reveal that AMY wrapped on CNT could induce the binding efficacy of PPs (atactic polypropylene (aPP), isotactic polypropylene (iPP) and syndiotactic polypropylene (sPP)) toward CNT by a significant reduction of distance between the center residue located on each amylose spiral and the adjacent one, especially for iPP and sPP systems. The radius of gyration shows that PPs spirally wrapped around CNT. Additionally, electrostatic attraction is found to be the main interaction inducing PPs to become spirally contacted with CNT. In case of CS modification, it can induce PPs binding but not in a spiral-shape on CS outer surface. The radius of gyration of PPs in CS modified CNT system conflicts with that of AMY model due to it interact with CNT/CS in snake-like shape of electrostatic interaction.

Field of Study:	Petrochemistry and	Student's Signature	
	Polymer Science	Advisor's Signature	
Academic Year:	2017	Co-Advisor's Signature	
		Co-Advisor's Signature	

ACKNOWLEDGEMENTS

จุฬาลงกรณ์มหาวิทยาลัย
CHULALONGKORN UNIVERSITY

CONTENTS

จุฬาลงกรณ์มหาวิทยาลัย

CHULALONGKORN UNIVERSITY

LIST OF FIGURES

LIST OF ABBREVIATIONS

4GA	alpha-D-glucose
AMY	amylose
aPP	atactic polypropylene
CS	chitosan
Cg	center of gravity
CG	conjugated gradient
CNT	carbon nanotubes
DD	degrees of deacetylation
ele	electrostatic
GAFF	General Amber Force Field
GlcN	glucosamine
GlcNA	n-acetyl glucosamine
iPP	isotactic polypropylene
MD	molecular dynamics
MWCNT	multi-walled carbon nanotube
PP	polypropylene
PBC	Periodic Boundary Conditions
PME	Particle Mesh Ewald
Rg	Radius of gyration
RMSD	root mean square displacement
SEM	scanning electron microscopy
SD	steepest descents
sPP	syndiotactic polypropylene
SWCNT	single-wall carbon nanotube
vdW	Van der Walls

Chapter I
INTRODUCTION

1.1 Background and rationale

Polymer/carbon nanotubes (CNTs) nanocomposites have been fabricated from its good processability characteristics of the polymer and excellent functional properties of the CNTs. The unique properties of CNTs are high electrical and thermal conductivity, excellent stiffness against bending and high tensile strength. Using CNTs as reinforcement can enhance the properties of polymer. Therefore, Polymer/CNTs nanocomposites are suitable for producing capacitor, car component and electrical component and etc. Although CNTs have excellent properties but, one of their disadvantages is aggregation of CNTs main by van der Waals interactions. This phenomenon results in the poor adhesive between polymer and CNTs. Polypropylene is the polymer that was selected for this study. To explore this problem, biopolymers particularly for amylose and chitosan can be used to reduce CNTs aggregation by wrapping the outer surface of CNTs. Moreover, amylose and chitosan can also improve the properties of isotactic polypropylene. Therefore, the aim of this project is to investigate the structural and interactions of biopolymers and CNT by means of molecular dynamics (MD) simulation in vacuum condition for 100 ns with Amber 16 program.

1.2 Literature reviews

Nanocomposite is a multiphase solid material in which at least one of the phases shows dimensions of less than 100 nanometers called "nanofillers" or "nanoparticles" [1]. The result of the addition of nanofillers in ceramic, metal or polymer can enhance the thermal and mechanical properties, including toughness and electrical and thermal conductivity. The examples of nanofillers added to composite are clay, gold particle and carbon nanotube [1-3]. Applications of nanocomposites can be used as capacitors, car components and in drug delivery [4, 5].

Carbon nanotubes (CNTs) are tube-shaped materials with diameter in nanometer scale and length up to several centimeters. They have high curvature and extra-large surface area. CNTs are composed of one carbon atom linked to three other carbon atoms by covalent bonds [6-8]. CNTs are attractive to research interests due to their unique properties such as high electrical and thermal conductivities, excellent stiffness against bending, high tensile strength, highly flexible, low mass density, very elastic and good electron field emitters [9-11]. They are made up from folding of graphene sheet, in which one sheet of graphene produces single-walled carbon nanotube (SWCNT) with diameter of around 0.4 nanometers, while the folding of multiple sheets becomes multi-walled carbon nanotube (MWCNT) with diameter of around 100 nanometer [2] (**Figure 1.1**).
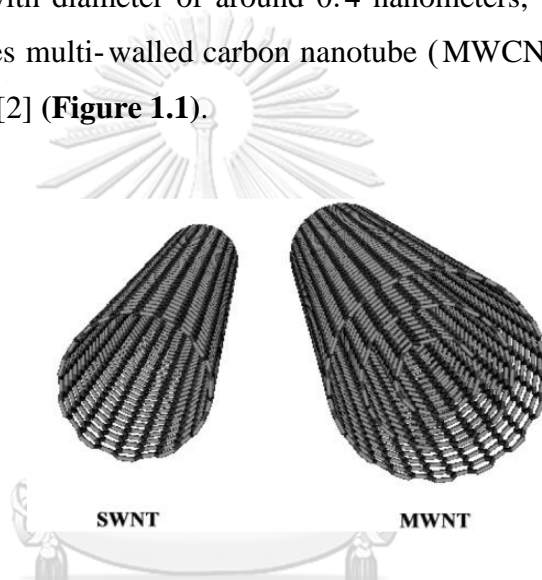
Figure 1.1 The 3D structures of single-walled and multi-walled carbon nanotubes

Polymer/CNT nanocomposites comprise a polymer or copolymer with CNT nanofiller. CNT is used as nanofiller in polymer for improving the mechanical, thermal and electrical properties of polymer [12-16]. In this work, the polypropylene (PP)/CNT nanocomposite is focused. PP is widely used in many industries due to its several beneficial properties, including low mass, high tensile strength and chemical resistance. However, it shows the low properties of thermal stability as well as electrical conductivity [17, 18]. Thus, the addition of CNT into polymer matrix is able to improve those properties. Deng and co-worker [19] investigated the dispersion of CNT in PP/CNT nanocomposite using scanning electron microscopy (SEM) (**Figure 1.2a**) and they found that CNTs were aggregated and showed a poor dispersion in polymer matrix, leading to a difficulty in synthesis of PP/CNT nanocomposite. Moreover Syamol and

co-worker [20] indicated that isotactic polypropylene (iPP) could poorly wrap around CNT outer surface and the intramolecular interactions between iPP units themselve were also found using molecular dynamics (MD) simulation (**Figure 1.2**).
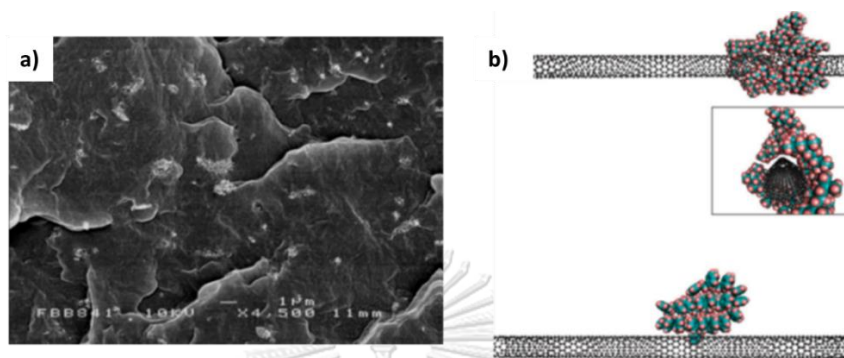
Figure 1.2 a) SEM image of PP/CNT nanocomposite and b) the last snapshot of PP/CNT system [19]

Biopolymers with notable chemical and biological properties are such as amylose (AMY) and chitosan (CS) [21]. AMY is formed by α-D-glucose units through α(1→4) glycosidic bonds [22-24]. Meanwhile chitosan is formed by a large sequence of glucosamine (GlcN) and n-acetyl glucosamine (GlcNA) units as shown in **Figure 1.3**. Zang and co-worker [25] added AMY, CS and the other polysaccharides into CNTs for investigation of cell behavior. They found that AMY and CS, which can wrap around CNT (**Figure 1.4**), led to a decrease in the CNT aggregation and enhance cell adhesion. In addition Xie and co-worker [26] studied the intermolecular interactions between AMY and CNT using MD simulations at 300 K. The results showed that AMY wrapped around CNT outer surface through van der waals interaction and it can encapsulate into CNT cavity. Aztatzi-Pluma and co-worker [27] used MD simulation for studying interactions between chitosan at different degrees of deacetylation (DD) and CNT at 300 K for 3.5 ns. They found that the interaction between the chitosan and the CNT are dependent on the %DD. The results from MD displayed that 60% DD of chitosan showed the strongest interaction with CNT because it has the lowest interaction energy. Rungrotmongkol and co-worker [4] suggested that chitosan can wrap around CNT main by van der Waals interaction.
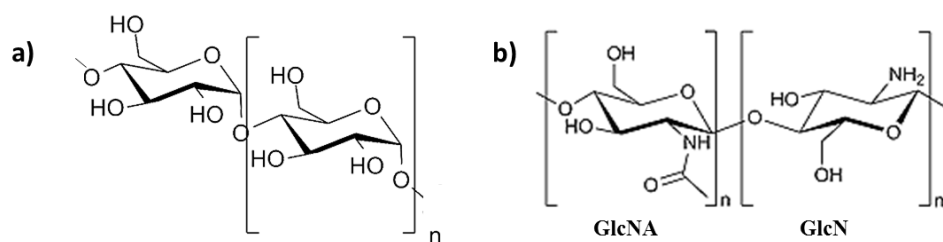
Figure 1.3 2D structures of a) amylose and b) chitosan
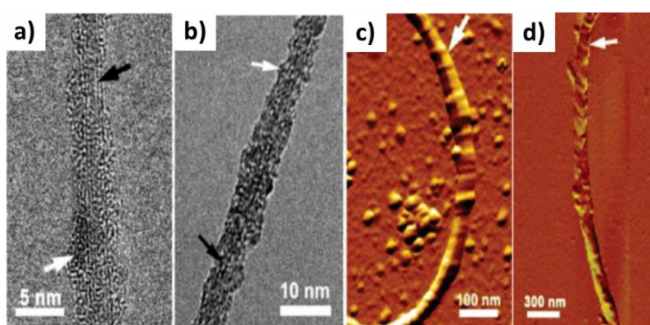
Figure 1.4 Transmission electron microscopy (TEM) image of a) amylose-CNT b) chitosan-CNT and Atomic force microscopy (AFM) image c) amylose-CNT and d) chitosan-CNT [25]

Basu and co-worker [28] investigated the blending of AMY/PP. They suggested that AMY can interact with PP, leading to an enhancement of melt flow index of PP. However, the information at molecular level regarding the main interaction of AMY with PP has not been well revealed. Furthermore Salmah and co-worker [29] studied properties of PP/chitosan nanocomposite by adding chitosan and modified chitosan into PP matrix. It was found that chitosan and modified chitosan increase in young modulus and thermal property. In addition, chitosan and modified chitosan interacted with PP. However, the lack of information about main interaction of amylose and chitosan with PP have not well understood. In this work, PP/CNT nanocomposite is focused to reduce CNT aggregation by wrapping biopolymers, i.e., AMY and CS, around its outer surface using MD simulation in vacuum condition with Amber 16 program for 100 ns.

1.3   Objectives of the study

To study the effect of AMY and CS non-covalently modified on SWCNT towards the binding of the three different PPs (aPP, iPP and sPP) using molecular dynamics simulation.

1.4   Scope of research

This thesis investigates the binding interactions, molecular dynamics behavior and binding affinities of AMY and CS with isotactic propylene/carbon nanotube nanocomposite by means of MD simulation for 100 ns in vacuum condition at 298 K.

1.5   Research procedures

1. Literature reviews
2. Prepare CNT, amylose, chitosan and polypropylene parameters by antechamber module
3. Build different models of amylose, chitosan, (10, 0)SWCNT and three typs of PPs (aPP, iPP and sPP).
   - Amylose, chitosan, PP and (10,0)SWCNT is built by tlEaP module implemented in AMBER16 package, and using GYCAM_06J-1 forcefield for construct amylose and chitosan.
4. Construct complexes of CNT/aPP, CNT/iPP, CNT/sPP, CNT/AMY/aPP, CNT/AMY/iPP, CNT/AMY/sPP, CNT/CS/aPP, CNT/CS/iPP and CNT/CS/sPP for MD simulation.
5. Simulate all systems with AMBER 16 at 298 K in vaccum condition for 100 ns
   5.1   Minimization: molecules were minimized with 3,000 steps of steepest descents (SD) and conjugated gradient (CG)
   5.2   Heating: The systems were heated till 298K temperature.
   5.3   Production: MD run at 298 ns for 100 ns
6. Analyze structural and dynamics properties as follows:

- Stability of all complex by root mean square displacement (RMSD) calculation
- Van der Walls (vdW) and electrostatic (ele) interaction energy
- Distance between center of gravity of CNT and center of gravity of each units of polymers
- Radius of gyration (Rg) of polymer

7.   Summary, and thesis and publication preparations

1.6   Expected beneficial outcome from the thesis

Molecular dynamics simulation information of biopolymer with polypropylene/CNT nanocomposite will be obtained and can be used to improve the adhesive of isotactic polypropylene to carbon nanotube.

จุฬาลงกรณ์มหาวิทยาลัย
CHULALONGKORN UNIVERSITY
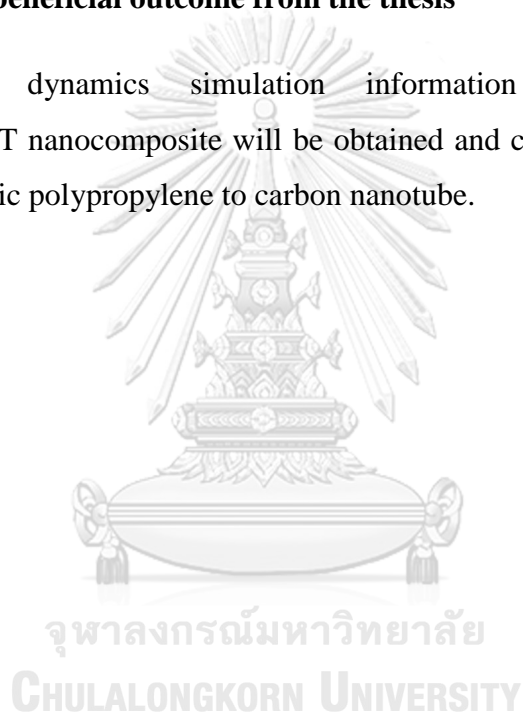
Chapter II
THEORIES

2.1   Molecular dynamics (MD) simulation

MD simulation is one of theory of computer simulation. In recent years computer simulation has become a major tool for material science, complementing both analytical theory and experimental. This interest is due both to the many fundamental scientific questions that material systems and to the technological importance of material science. So, MD simulation is used to assist to experimental limitations, such as experimental processes are difficult, expensive, and takes a long time. The equations of motion follow from Newton's second law [30]. Fundamentally, the acceleration of particles can be calculated by the first-order derivative of velocity (V_i) or second-order derivative of the atomic position (r_i) with respect to time t (eq.1).

$$F_i = m_i a_i = m_i \frac{dV_i}{dt^2} = m_i \frac{d^2 r_i}{dt^2} \tag{1}$$

Where F_i is the total force exerted on the particle i

m_i is mass of the particle i

a_i is acceleration of the particle i at

t is time

In addition, the external force acting on the particle i can be obtained from the negative gradient of potential energy (U) [31] as shown in eq. 2

$$F_i = -\frac{d}{d_{r_i}} U \tag{2}$$

Combination of all mentioned equation leads us to obtain (eq. 3)

$$F_i = -\frac{d}{d_{r_i}} U = m_i a_i = m_i \frac{dV}{dt} = m_i \frac{d^2 r_i}{dt^2} \tag{3}$$

In molecular system, the potential energy is the summation between the bonded and non-bonded interactions of particles. Bonded interactions compose of covalent

bond-stretching, angle-bending, and dihedral angle potentials as described by harmonic oscillator function. Meanwhile, non-bonded interactions consist of electrostatic (ele) and van der Waals (vdW) interactions, which are described by coulomb potential and Lennard-Jones (L-J) potential, respectively. The sum of potential energy interaction can be expressed as follows:

$$U = E_{bonded} + E_{non\text{-}bonded} \tag{4}$$

$$U = (E_{bonds} + E_{angles} + E_{dihedrals})_{bonded} + (E_{ele} + E_{vdW})_{non\text{-}bonded} \tag{5}$$

$$U = \sum_{bonds} \frac{1}{2}k_b(r\text{-}r_{eq})^2 + \sum_{angles} \frac{1}{2}k_\Theta(\Theta\text{-}\Theta_{eq})^2 + \sum_{dihedrals} \frac{1}{2}V_n(1 + \cos(n\phi\text{-}\gamma)) \tag{6}$$

$$+ \sum_{i<j}^{atoms} \frac{q_i q_j}{D r_{ij}} + \sum_{i<j}^{atoms} \left(\frac{A_{ij}}{r_{ij}^{12}} - \frac{B_{ij}}{r_{ij}^{6}} \right)$$

Where k_b is the force constants for bond-stretching

$\quad k_\Theta$ is the force constants for angle-bending

$\quad r_{eq}$ is the equilibrium bond length

$\quad \Theta_{eq}$ is bond angle

$\quad V_n$ is the height of rotational barrier

$\quad n$ is the periodicity of rotation

$\quad \phi$ is the dihedral angle in the conformation of molecule in the phase shift angle, γ.

As previously mentioned, the non-bonded energy accounts for the electrostatic and van der Waals energies of the pair-wise sum of all possible interactions on atoms i and j. An electrostatic energy relies on the Coulomb's law which corresponds to the atomic charges, q_i and q_j, of atom i and j, respectively. Whereas, D is the effective dielectric constant. The van der Waals interactions are commonly used to describe steric interactions of molecule. Typically, the van der Waals energy is the sum of the attraction and repulsion between particles. The attractive interaction of van der Waals rapidly occurs in a short-range proportional to $1/r^6$ of the L-J potential. While the repulsion occurs with distance of interacting atoms become slightly less than the sum of their radius determined by the proportion of $1/r^{12}$. The A_{ij} and B_{ij} are constant factors

which are dependent on the specific type of atom *i* and *j*. The position and velocity of atoms based on equation of motion can be calculated at time $t+\Delta t$.

2.2 The MD Algorithm

There are various algorithms such as Verlet algorithm, leapfrog algorithm, velocity Verlet algorithm etc. All algorithms are used for approximating the positions, velocities and accelerations with Taylor's expansion can be expressed as following equations 7-9:

$$r(t+\Delta t) = r(t) + v(t)\Delta t+ \frac{1}{2}a(t)\Delta t^2 + \dots \tag{7}$$

$$v(t+\Delta t) = v(t) + a(t)\Delta t + \frac{1}{2}b(t)\Delta t^2 + \dots \tag{8}$$

$$a(t+\Delta t) = a(t) + b(t)\Delta t + \dots \tag{9}$$

The algorithm which is commonly used for molecular modeling is the Verlet algorithm, as shown in equations 10 and 11

$$r(t + \Delta t) = r(t) + v(t)\Delta t+ \frac{1}{2}a(t)\Delta t^2 \tag{10}$$

$$r(t + \Delta t) = r(t) - v(t)\Delta t+ \frac{1}{2}a(t)\Delta t^2 \tag{11}$$

with combinations of these two equations, one gets

$$r(t + \Delta t) = 2r(t) - r(t - \Delta t)+ a(t)\Delta t^2 \tag{12}$$

This technique determines the new position at time $t + \Delta t$ or $t - \Delta t$ from the current position and acceleration
However, algorithm that default of AMBER program is leapfrog algorithm. The leap frog scheme is equivalent to the Verlet algorithm, but solves for the velocities at half time step intervals:

$$v(t + \frac{\Delta t}{2}) = v(t - \frac{\Delta t}{2}) + \frac{f(t)}{2m}\Delta t \tag{13}$$

$$r(t + \Delta t) = r(t) + v(t + \frac{\Delta t}{2}) \Delta t \tag{14}$$

leap frog approach is that the velocities are not known at the same time as the positions, making it difficult to evaluate the total energy (kinetic + potential) at any one point in time. We can get an estimate from:

$$v(t) = \frac{v\left(t + \frac{\Delta t}{2}\right) + v(t - \frac{\Delta t}{2})}{2} \tag{15}$$

2.3   Particle mesh Ewald (PME) method

Ewald summation was developed as a method in theoretical physics, long before the advent of computers. The Ewald summation method is a conventional method for computing the electrostatic interaction in a periodic boundary condition. Total electrostatic energy, including the contribution from the image cells. In the particle mesh method, just as in standard Ewald summation, the generic interaction potential is separated into two terms. The basic idea of particle mesh Ewald summation is to replace the direct summation of interaction energies between point particles.

$$E_{TOT} = E_{sr} + E_{lr} \tag{16}$$

with two summations, a direct sum E_{sr} of the short-ranged potential in real space

$$E_{sr} = \sum_{i,j} \varphi(r_j - r_i) \tag{17}$$

that is the particle part of particle mesh Ewald) and a summation in Fourier space of the long-ranged part

$$E_{lr} = \sum_k \phi_{lr}(k)|\rho(k)|^2 \tag{18}$$

where ϕ_{lr} and $\rho(k)$ represent the Fourier transforms of the potential and the charge density (that's the Ewald part). Since both summations converge quickly in their respective spaces (real and Fourier), they may be truncated with little loss of accuracy and great improvement in required computational time. To evaluate the Fourier transform $\rho(k)$ of the charge density field efficiently, one uses the Fast Fourier transform, which requires that the density field be evaluated on a discrete lattice in space.

2.4   Cutoff distance

All non-bonded pair interactions acting on the i atom over the containing millions atoms in simulation system takes a very computational expense. To overcome this limitation, the non-bonded terms in van der Waals and electrostatic are considerably truncated in more compacted region called cutoff radius, to reduce the time-consuming of MD simulation. Normally, the cutoff limit is set around 10-12 Å centered on the focusing atom. An applied cutoff may not have accuracy of the calculated forces, however, other rest atoms are assumed to have less effect due to too long length.

2.5   Periodic Boundary Conditions (PBC)

Small sample size means that, unless surface effects are of particular interest, periodic boundary conditions need to be used. Consider 1000 atoms arranged in a $10 \times 10 \times 10$ cube. Nearly half of the atoms are on the outer faces, and these will have a large effect on the measured properties. Even for $10^6 = 100^3$ atoms, the surface atoms amount to 6% of the total, which is still nontrivial. Surrounding the cube with replicas of itself takes care of this problem. Provided the potential range is not too long, we can adopt the *minimum image convention* that each atom interacts with the nearest atom or image in the periodic array. In the course of the simulation, if an atom leaves the basic simulation box, attention can be switched to the incoming image. This is shown in **Figure 2.1**. Of course, it is important to bear in mind the imposed artificial periodicity when considering properties which are influenced by long-range correlations.
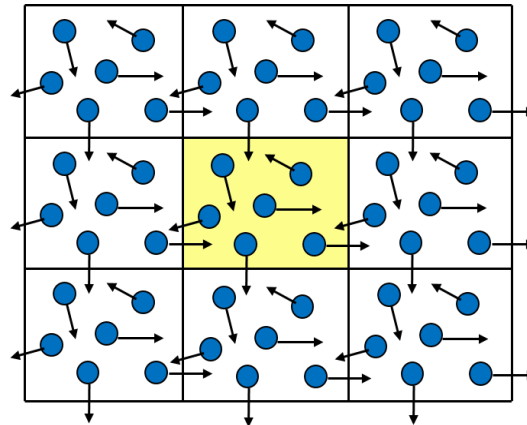
Figure 2.1 Periodic boundary conditions. As a particle moves out of the simulation box, an image particle moves in to replace it.

2.6 Root mean square deviation (RMSD)

The stability of MD systems was analyzed by Root mean square deviation (RMSD). RMSD is a measure of the different coordinates between MD structures at time respected to initial structure. The RMSD of atoms is calculated by three coordinates (x, y, z) shown in equation 19:

$$\langle u^2 \rangle = \sqrt{\frac{1}{n}\sum_{i=1}^{n}((a_{ix} - b_{ix})^2 + (a_{iy} - b_{iy})^2 + (a_{iz} - b_{iz})^2} \qquad (19)$$

where $\langle u^2 \rangle$ is mean square displacement of atoms

n is atoms of molecule

a and b are coordinate at points of starting and MD production

2.7 Radius of gyration of polymers (Rg)

The radius of gyration (Rg) calculation was used to identify the mean squared distance of each point on the molecule from its center of gravity using equation 20:

$$Rg = \sqrt{\frac{1}{N}\sum_{N}^{i=0}(r_i - r_m)^2}$$ (20)

Where N is the number of atoms

r$_i$ denotes atomic position

r$_m$ denotes the mean position of all atoms

2.8   Electrostatic (ele) and Van der Waals (vdW) interaction energy

In this study using pairwise in cpptraj to calculate the van der waals (vdW) and electrostatic (ele) interaction. This option has two related functions: 1) Calculate pairwise energy (in kcal/mol) or 2) Compare pairwise energy of frames to a reference frame. Both interaction energy can be calculated by equations 21 and 22:

$$\Delta E_{ele} = \sum_{i<j}^{atoms} \frac{q_i q_j}{D r_{ij}}$$ (21)

$$\Delta E_{vdW} = \sum_{i<j}^{atoms} \left(\frac{A_{ij}}{r_{ij}^{12}} - \frac{B_{ij}}{r_{ij}^6} \right)$$ (22)

Where i and j are atoms, which corresponds to the atomic charges,

q_i and q_j, are atomic charge of atom i and j, respectively

D is the effective dielectric constant.

CHAPTER III
RESEARCH METHODOLOGY

3.1 Molecular models of amylose (AMY), chitosan (CS), polypropylene (PP) and carbon nanotube (CNT)

The 3D structure of AMY containing 30 units of alpha-D-glucose (4GA residue) was constructed using the tLEaP module implemented in AMBER 16. In case of 3D structure of CS, it has two models which consist of 30 (30CS) and 50 (50CS) units and are generated by tLEaP module. All models of CS are the neutral with 60 %DD. The three types of polypropylene (PP), including atactic polypropylene (aPP), isotactic polypropylene (iPP) and syndiotactic polypropylene (sPP) consisting of 30 repeating units of PP were generated using the Material Studio 5.5 Suite. Note that, the methyl groups are randomly positioned in aPP form, whereas the methyl groups are constructed along the same side and alternate side of the polymer chain in iPP and sPP systems, respectively. The (10,0) zigzag of single-walled CNT with a diameter of 7.8 Å, chiral vectors n = 10 and m = 0, containing 30 repeating units was built using the Material Studio 5.5 Suite. Subsequently, the CNT was wrapped spirally with amylose in according to the previous research [26]. AMY was parameterized by Glycam_06j-1 force field [32], while all PPs and CNT were treated by the General Amber Force Field (GAFF) [33]. In total, there are twelve generated systems without and with AMY and two length of CS including *system i:* CNT/aPP; *system ii:* CNT/iPP; *system iii:* CNT/sPP; *system iv:* CNT-aPP wrapped with amylose (CNT/AMY/aPP); *system v:* CNT-iPP wrapped with amylose (CNT/AMY/iPP); *system vi:* CNT-sPP wrapped with amylose (CNT/AMY/sPP); *system vii and viii* CNT-aPP wrapped with two length of CS (CNT/30CS/aPP and (CNT/50CS/aPP; *system ix and x* CNT-iPP wrapped with two length of CS (CNT/30CS/iPP and (CNT/50CS/iPP) and *system xi and xii* CNT-sPP wrapped with two length of CS (CNT/30CS/sPP and (CNT/50CS/sPP). Each PP was placed in parallel with the length (x axis) of CNT as shown in **Figure 3.1** and **3.2**
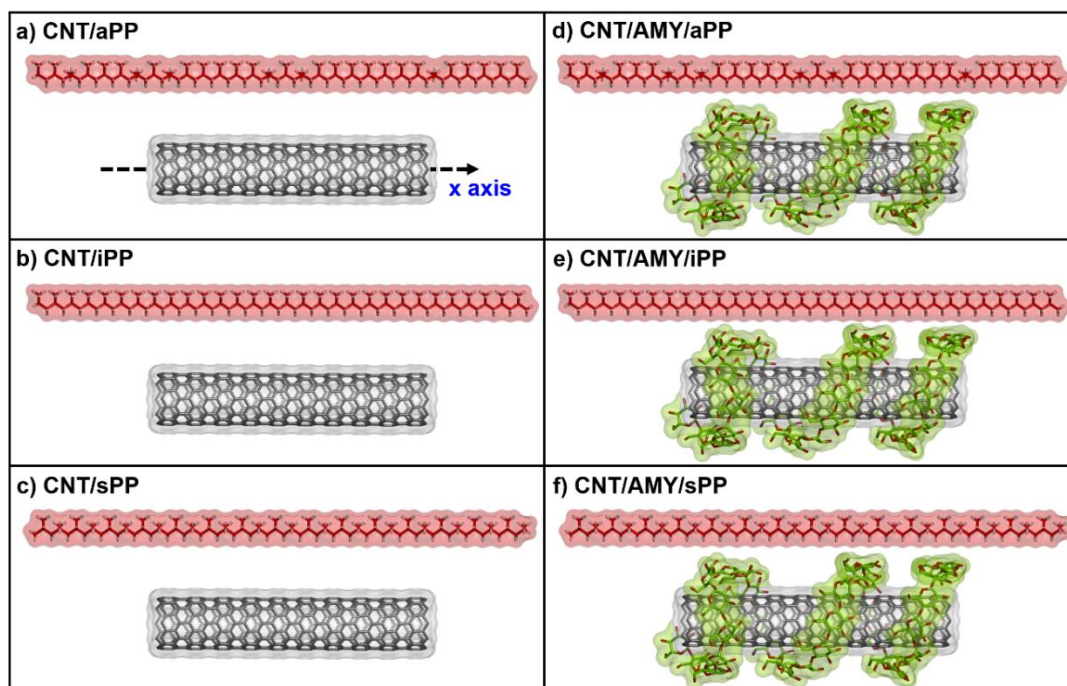
Figure 3.1 The initial structures of CNT/PPs nanocomposite without and with AMY modification for MD study: a) CNT/aPP, b) CNT/iPP and c) CNT/sPP d) CNT/AMY/aPP, e) CNT/AMY/iPP and f) CNT/AMY/sPP. PP (red) was placed in parallel with the X axis of CNT and AMY (green) was spirally wrapped around CNT surface.
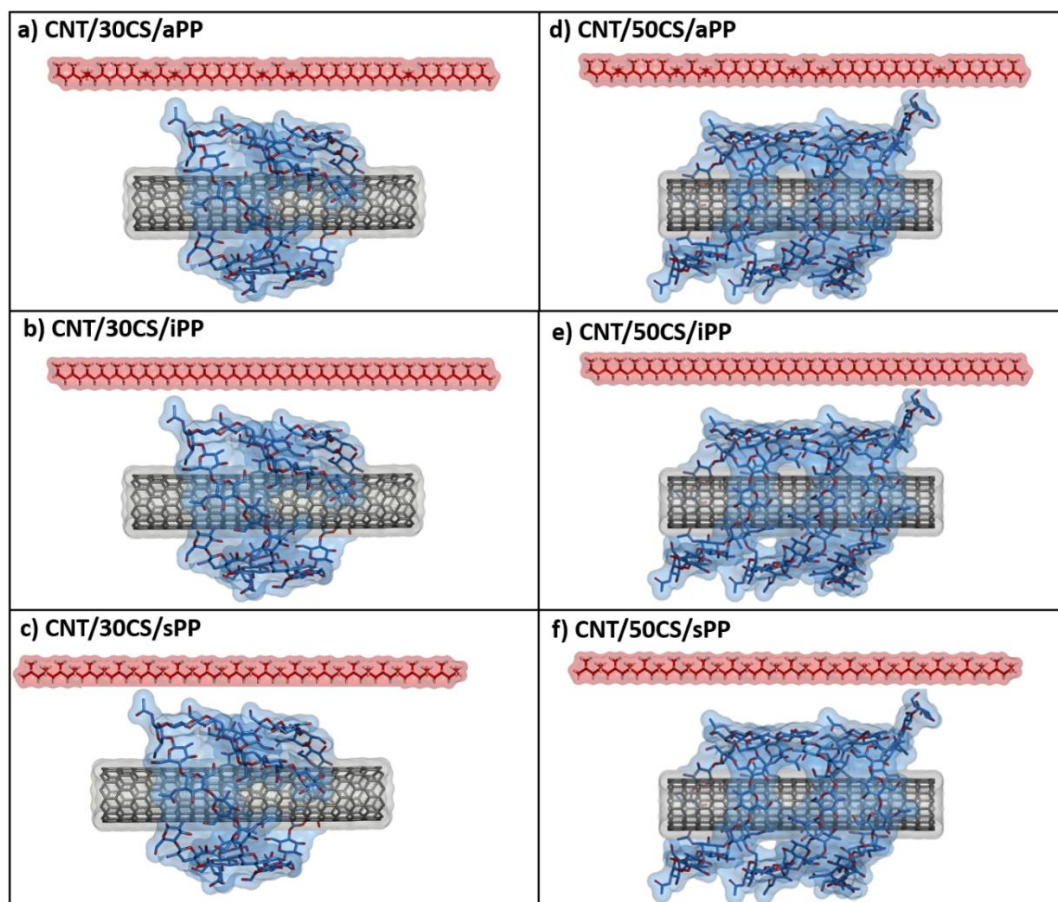
Figure 3.2 The initial structures of CNT/PPs nanocomposite with CS modification for MD study: a) CNT/30CS/aPP, b) CNT/30CS/iPP and c) CNT/30CS/sPP d) CNT/50CS/aPP, e) CNT/50CS/iPP and f) CNT/50CS/sPP. PP (red) was placed in parallel with the X axis of CNT and CS (light blue) was spirally wrapped around CNT surface.

3.2   Molecular dynamics (MD) simulation

MD simulation was performed under vacuum condition using AMBER16 package with the *NPT* ensemble at 1 atm and 298 K using a time step of 2 fs. The SHAKE algorithm [34] was applied to all bonds involving hydrogen atoms. The long-range electrostatic interactions were calculated using the Particle Mesh Ewald (PME) summation method [35]. Prior perform MD simulation, the hydrogen atoms were minimized with 3,000 steps of steepest descents (SD) and conjugated gradient (CG). All systems were heated up to 298 K for 100 ps and equilibrated at 298 K for 5 ns. Finally, the production stage was performed until 100 ns and the structural coordinate was saved every 2 ps for analysis. The root-mean square displacement (RMSD), radius of gyration, and van der Waals and Electrostatic interactions were calculated by the cpptraj module [36] implemented in AMBER16 while the distance between the centers of gravity of each polymer unit and CNT was computed with FORTRAN script [5].

จุฬาลงกรณ์มหาวิทยาลัย
CHULALONGKORN UNIVERSITY
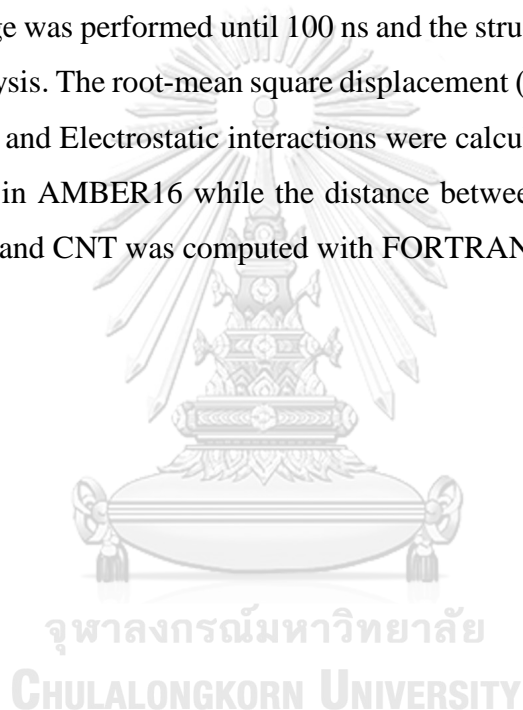
CHAPTER IV
RESULTS AND DISCUSSION

4.1 System stability

- The CNT/PPs systems without and with AMY non-covalent modification CNT surface

To estimate the system stability of the CNT/PPs nanocomposites without and with AMY non-covalent modification on the external surface of single-walled CNT, the root-mean-square displacement (RMSD) of each system relative to the minimized structure was calculated along the simulation time and plotted in **Figure 4.1** The RMSD values of PP (dark green) of three systems without amylose wrapping (**Figure 4.1a-c**), including CNT/aPP, CNT/iPP and CNT/sPP, rapidly increase at the first 60 ns and fluctuate in the range of ~16-20 Å until the end of the simulations. In case of AMY wrapped on CNT, the RMSD values of PP showed relatively lower fluctuation and reached the equilibrium state after ~ 40 ns for the CNT/AMY/iPP and CNT/AMY/sPP systems (**Figure 4.1e-f**) and 60 ns for the CNT/AMY/aPP system (**Figure 4.1d**). This is in contrast to AMY, in which the RMSD of 6 Å compared to its initial structure with a very low fluctuation was observed along the simulations in these three systems. As expected, no structural change of CNT was detected as seen by RMSD close to 0 Å. Taken together, all six studied systems seem to enter the equilibrium state at ~ 60 ns and thus the atomic coordinates in the last 40 ns were collected for further analysis.
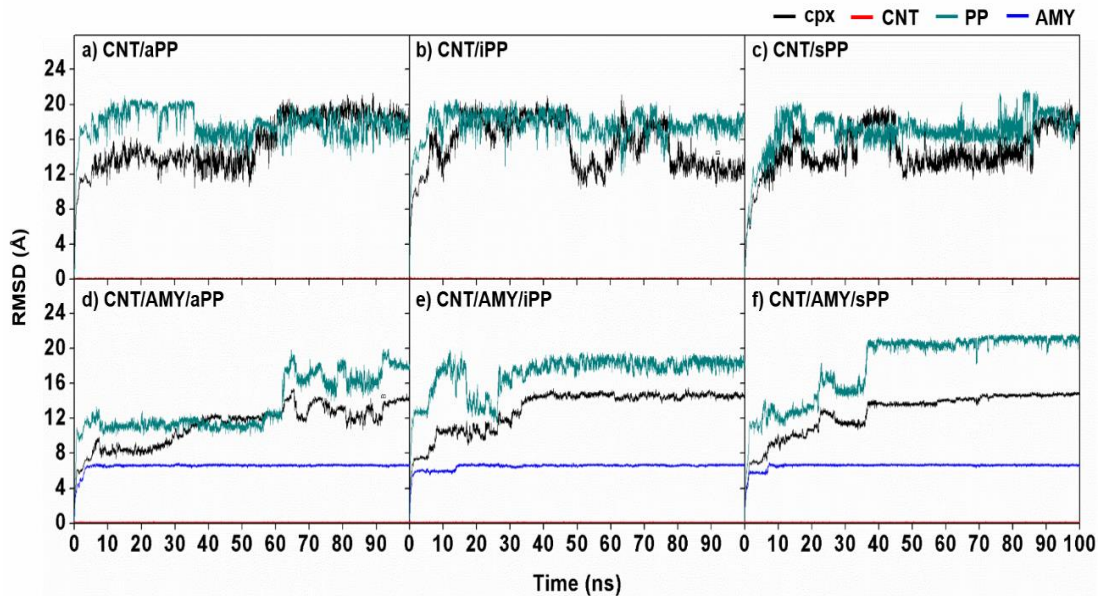
Figure 4.1 All-atom RMSDs of complex (black), CNT (red), PP (dark green) and AMY (blue) relative to their initial structures for the six studied systems: a) CNT/ aPP, b) CNT/ iPP and c) CNT/ sPP d) CNT/ AMY/ aPP, e) CNT/ AMY/ iPP and f) CNT/AMY/sPP.

- *The CNT/PPs systems with different length CS non-covalent modification CNT surface*

To measure the system stability of the CNT/PPs nanocomposites with different length CS non-covalent modification on the external surface of single-walled CNT, the RMSD value of each system relative to the minimized structure was calculated along the simulation time and plotted in **Figure 4.2** The RMSD values of PP (dark green) of all systems, rapidly increase at the first 10 ns and fluctuate in the range of ~11-12 Å until the end of the simulations. In the same way, RMSD of CS of all systems fluctuate in the range of ~4-6 Å, compared to its initial structure with a very low fluctuation was observed along the simulations. In case of CNT, no change was observed as seen in RMSD analysis which is close to 0 Å. The four systems, there are CNT/30CS/aPP, CNT/30CS/iPP, CNT/30CS/sPP and CNT/50CS/iPP seem to enter the equilibrium state at ~ 40 ns. But the two systems, consist of CNT/50CS/aPP and CNT/50CS/sPP reach

the equilibrium state at ~60 ns. Therefore, the atomic coordinates in the last 40 ns were collected for further analysis.
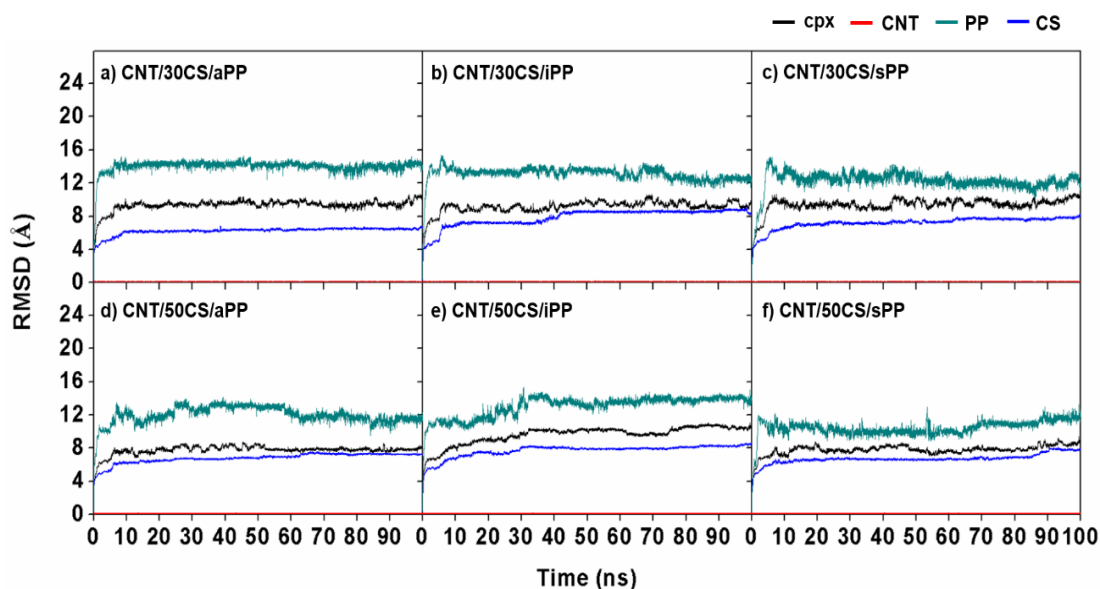

Figure 4.2 All-atom RMSDs of complex (black), CNT (red), PP (dark green) and CS (blue) relative to their initial structures for the six studied systems: a) CNT/30CS/aPP, b) CNT/30CS/iPPand c) CNT/30CS/sPP d) CNT/50CS/aPP, e) CNT/50CS/iPP and f) CNT/50CS/sPP.

4.2   Effect of AMY and CS on polypropylene binding toward carbon nanotube

The final orientation of PPs and AMY wrapped on CNT taken from the last MD snapshot of each system is depicted in **Figure 4.3** In case of no AMY modification on CNT, the results reveal that all three PPs preferentially interact within themselves, resulting in a non-spiral shape (**Figure 4.3a-c**). This observation strongly correlated with previous studies [20, 37, 38]. Interestingly, the AMY conjugating on CNT could enhance the efficacy of PPs bindings to become significantly to locate closer towards CNT with a formation of a spiral-shaped structure of PPs (**Figure 4.3d-f**). This process occurred by a significant reduction of distances between the center residue located on each amylose spiral and the adjacent one, resulting in a compact molecular structure, which facilitates the space for PPs recognition to interact with either AMY or CNT. In the CS modification on CNT surface systems, all PPs cannot wrap CNT in spiral-shape,

but the most of PP units wrapped on the CS outer surface better than directly wrapped CNT surface.
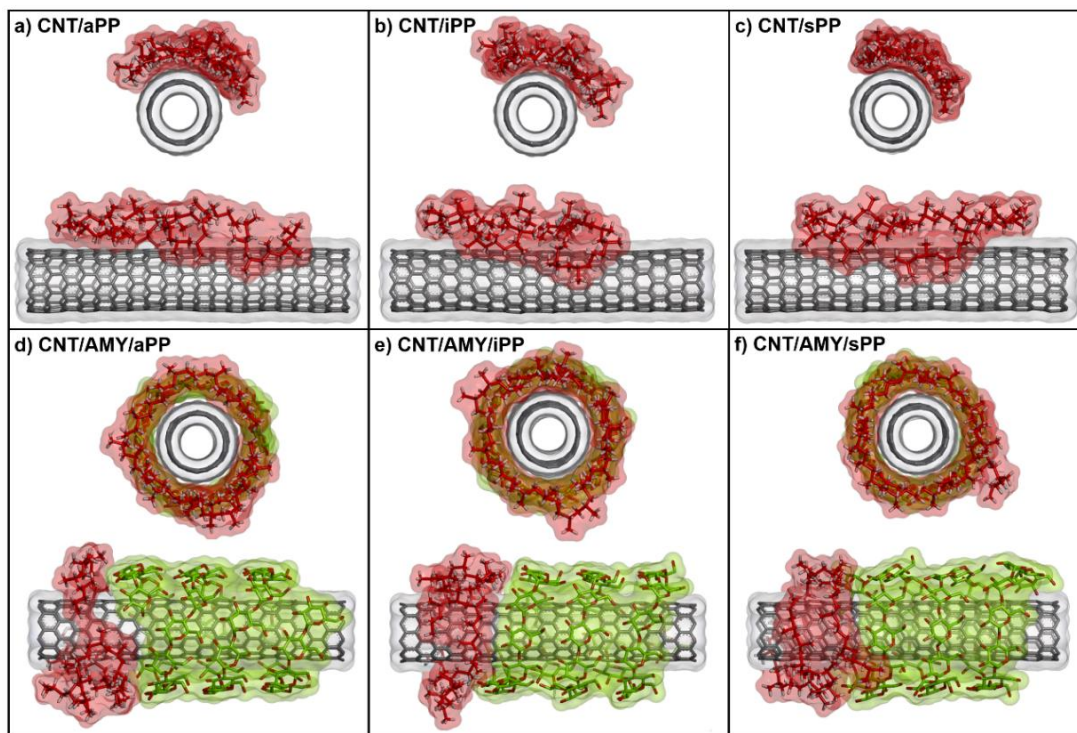
Figure 4.3 The last MD snapshots of a) CNT/ aPP, b) CNT/ iPP, c) CNT/ sPP, d) CNT/AMY/aPP, e) CNT/AMY/iPP and f) CNT/AMY/sPP systems, where PP and AMY structures are shaded by red and green.
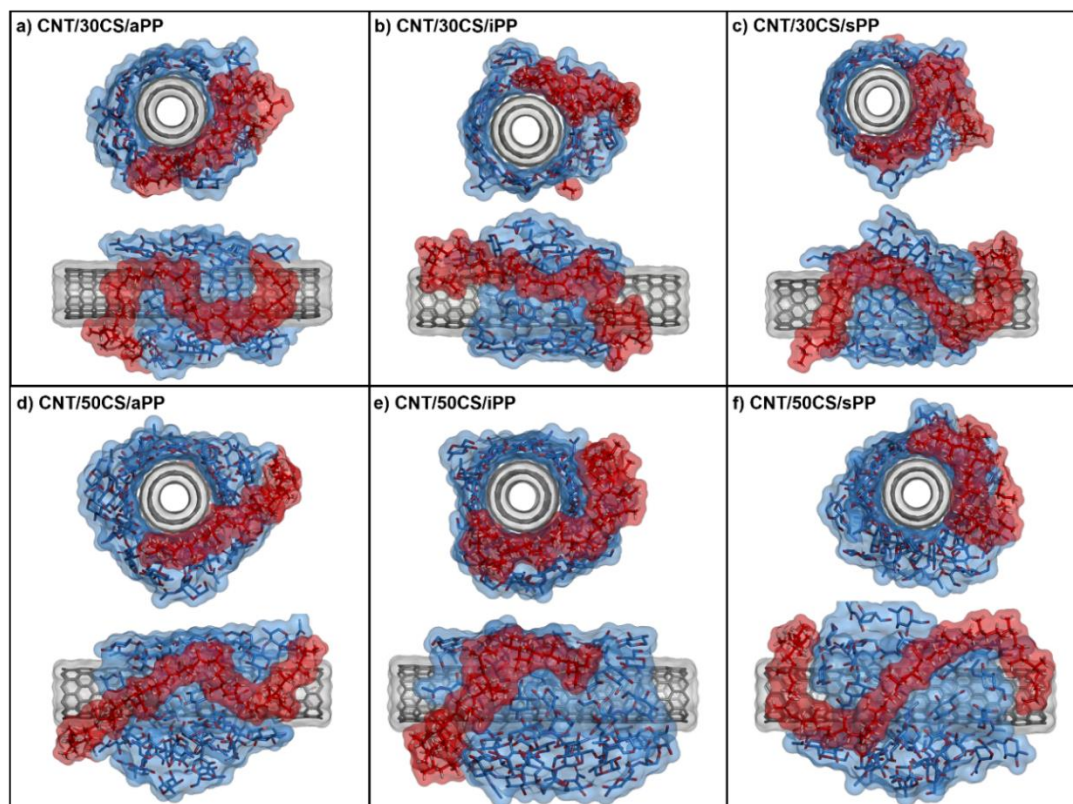
Figure 4.4 The last MD snapshots of a) CNT//30CS/aPP, b) CNT/30CS/iPP, c) CNT/30CS/sPP, d) CNT/50CS/aPP, e) CNT/50CS/iPP and f) CNT/50CS/sPP systems, where PP and AMY structures are shaded by red and light blue.

4.3 The averaged distance measured from Cg of PP and AMY units to surface of CNT

- The CNT/PPs systems without and with AMY non-covalent modification CNT surface

Furthermore, in order to compare the binding capacity between PPs toward CNT without and with AMY conjugation on the external surface, the distances measured from the center of gravity (Cg) of each unit of PPs to surface of CNT (d(PP_{Cg}-$CNT_{Surface}$)) averaged over the last 40 ns were calculated in relative to the distance measured from Cg of each AMY unit to surface of CNT (d(AMY_{Cg}-$CNT_{Surface}$)). These distances versus simulation time are plotted and given in **Figure 4.5** It can be clearly seen that all AMY units well interacted with the CNT outer surface with the averaged d(AMY_{Cg}-$CNT_{Surface}$) not exceed 5 Å (**Figure 4.5a**). The AMY

wrapping could importantly decrease the averaged d(PP$_{Cg}$- CNT$_{Surface}$) for the iPP and sPP systems from ~7 Å (**Figure 4.5b**) to ~3 Å (**Figure 4.5c**) for the systems without and with AMY non-covalently modified on CNT surface. However, only the 10 aPP units of one end exhibited a similar tight binding on the CNT/AMY whilst the rest units show a high fluctuation as detected which study. Taken together, the use of conjugated AMY on CNT exterior leads to an enhanced interfacial adhesion of PPs toward CNT, which is in a good agreement with the electrostatic and van der Waals attractions as discussed later.
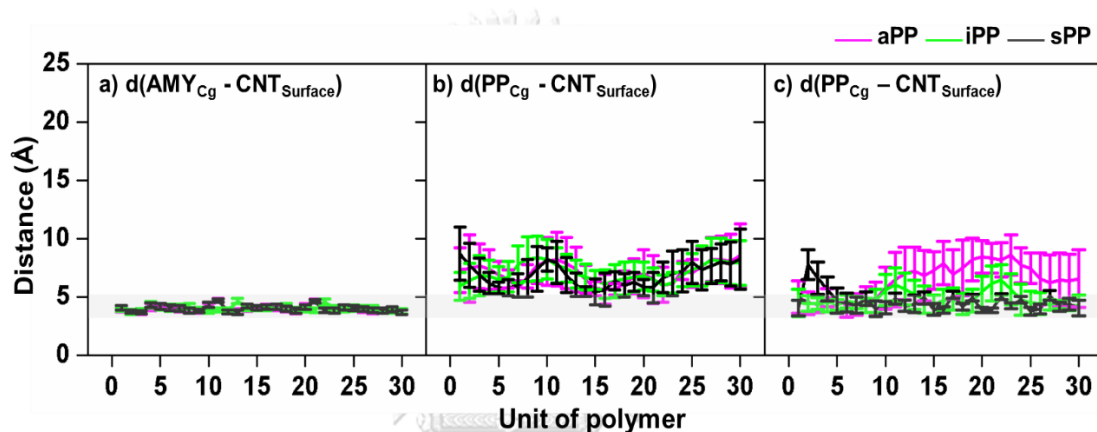
Figure 4.5 Plots of a) the averaged distance measured from Cg of each AMY unit to surface of CNT (d(AMY$_{Cg}$- CNT$_{surface}$)), and the averaged distance measured from Cg of each PP unit to surface of CNT (d(PP$_{Cg}$- CNT$_{Surface}$)) for the systems b) without and c) with AMY modified CNT surface

- The CNT/PPs systems with different length CS non-covalent modification CNT surface

The average distances from the center of gravity (Cg) of each unit of PP surface of CNT (d(PP$_{Cg}$- CNT$_{Surface}$)) at last 40 ns were calculated in relative to the distance measured from Cg of each different length CS unit surface of CNT (d(30CS$_{Cg}$-CNT$_{Surface}$) and d(50CS$_{Cg}$- CNT$_{Surface}$)). The results shown in **Figure 4.6,** d(30CS$_{Cg}$-CNT$_{Surface}$) and d(50CS$_{Cg}$- CNT$_{Surface}$)) (**Figure 4.6a,c**) have the distance in range of 3.5-10 Å and 3.5-11 Å respectively. In addition, d(PP$_{Cg}$- CNT$_{Surface}$) of the system 30 and 50 CS units are in range of 8-16 Å and 5-18 Å respectively.
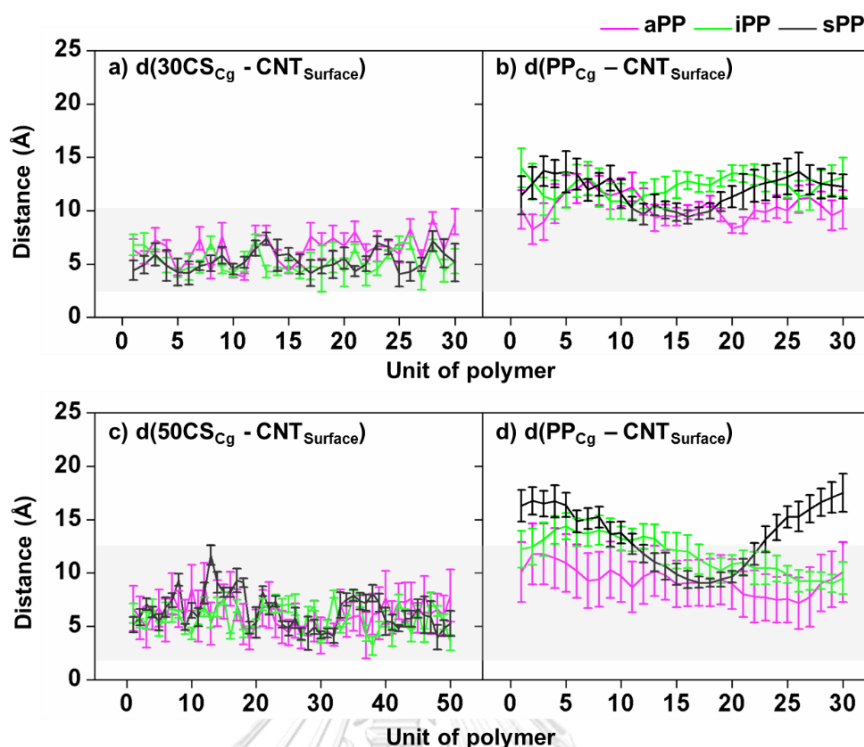
Figure 4.6 Plots of a) and c) the averaged distance measured from Cg of each 30CS and 50CS units to surface of CNT in the x axis (d(CS_{Cg}- $CNT_{Surface}$)), and the averaged distance measured from Cg of each PP unit to surface of CNT in the x axis (d(PP_{Cg}- $CNT_{Surface}$)) for the systems b) without and d) with different repeating units of CS modified CNT surface

4.4   Radius of gyration of polymers (Rg)

The radius of gyration (Rg) calculation was used to identify the mean squared distance of each point on the polymer, PP or AMY, from its center of gravity [39].In case of no conjugated AMY on CNT (**Figure 4.7a-c**), the Rg of all three PPs dramatically reduce within the first 20 ns and consequently retain fluctuated of ~8-11 Å until the end of simulation. This is because PPs preferentially interact with each other rather than spirally contact with CNT as described above. Interestingly, the use of AMY non-covalently modified on CNT significantly increases the Rg stability of iPP and sPP after 40 ns (**Figure 4.7e-f**), reflecting the stable conformation of partial spiral form for these PPs. However, in the aPP system **(Figure 4.7d)**, the Rg fluctuation is similar to

that of no AMY conjugation due to the high flexibility of one terminal end (**Figure 4.5d**), which was also reported previously [37]. Note that, the Rg plots of AMY are likely comparable for all three systems (**Figure 4.7d-f**), which was significantly lower than those of PPs in terms of value and fluctuation. On the other hand, Rg of different length CS non-covalently modified on CNT shown in **Figure 4.8**, Rg of CS of all systems is rapidly decrease at first 5 ns of simulation. Rg of PP is higher than CS because PP cannot wrap CNT surface in spiral-shape.
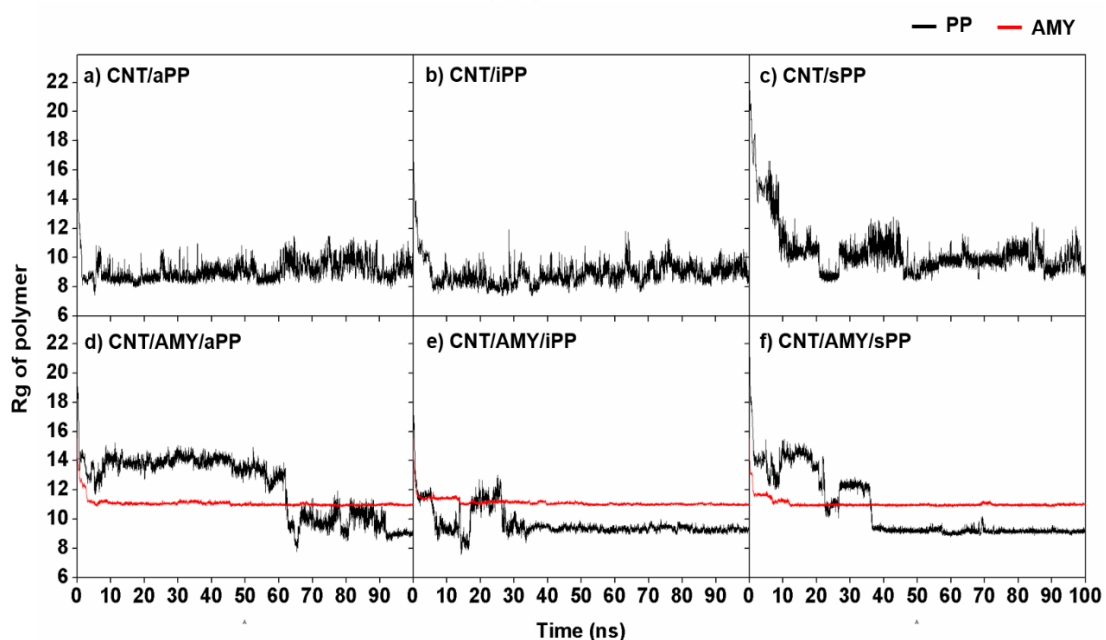
Figure 4.7 Plots of Radius of gyration (Rg) of polymers, PP (black) and AMY (red), versus simulation time for a) CNT/aPP, b) CNT/iPP, c) CNT/sPP, d) CNT/AMY/aPP, e) CNT/AMY/iPP and f) CNT/AMY/sPP systems.
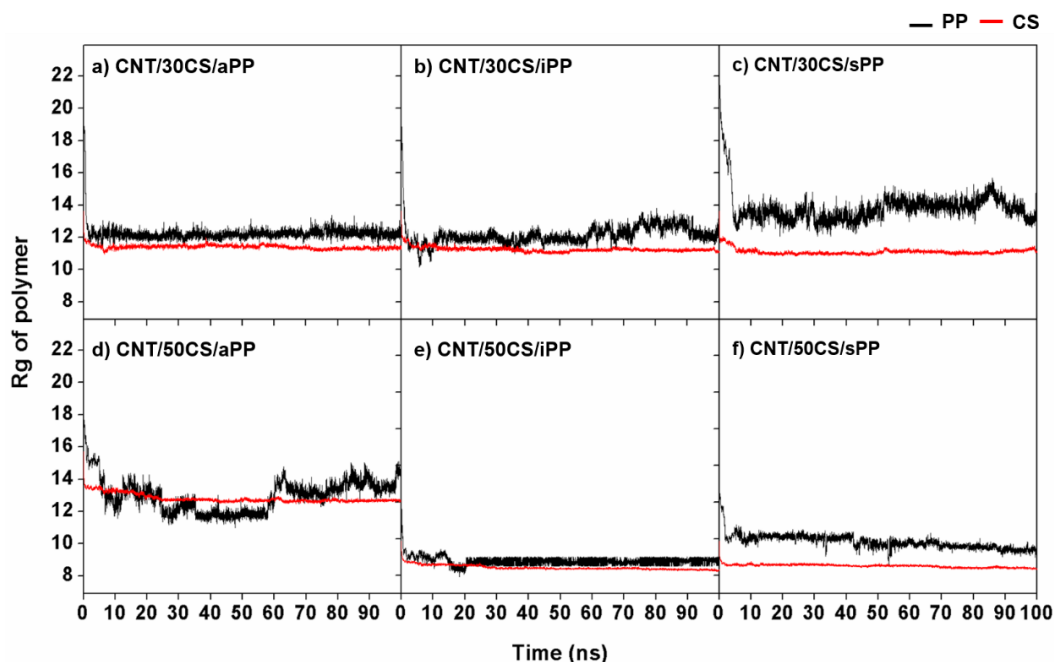
Figure 4.8 Plots of Radius of gyration (Rg) of polymers, PP (black) and AMY (red), versus simulation time for a) CNT/30CS/aPP, b) CNT/30CS/iPP, c) CNT/30CS/sPP, d) CNT/50CS/aPP, e) CNT/50CS/iPP and f) CNT/50CS/sPP systems.

4.5 Distance of end-to-end chain of polypropylene

In order to characterize the distance of end-to-end chain of PPs upon the molecular complexation toward CNT for both without and with AMY and CS modification on tube exterior, the distance of end-to-end chain of PPs was measured between center of gravity of the first unit of PP and center of gravity of the last unit of PP from all simulation. The results of the systems without and with AMY are plotted and compared in **Figure 4.9** As expected, in the iPP and sPP systems, the AMY wrapping enhances to the spiral form of PPs, whilst more distance of end-to-end chain was observed in the aPP system. It confirms that aPP is less spiral. In case of the systems without AMY, demonstrated that the distance is higher than systems with AMY due to PPs which is not spiral-shape and also at the end chain of PP. Considering the systems modified by different length CS (**Figure 4.10**), the distance of end-to-end chain of PPs are higher than CNT modified by AMY. It confirms the non-spiral-shape of PPs**.**
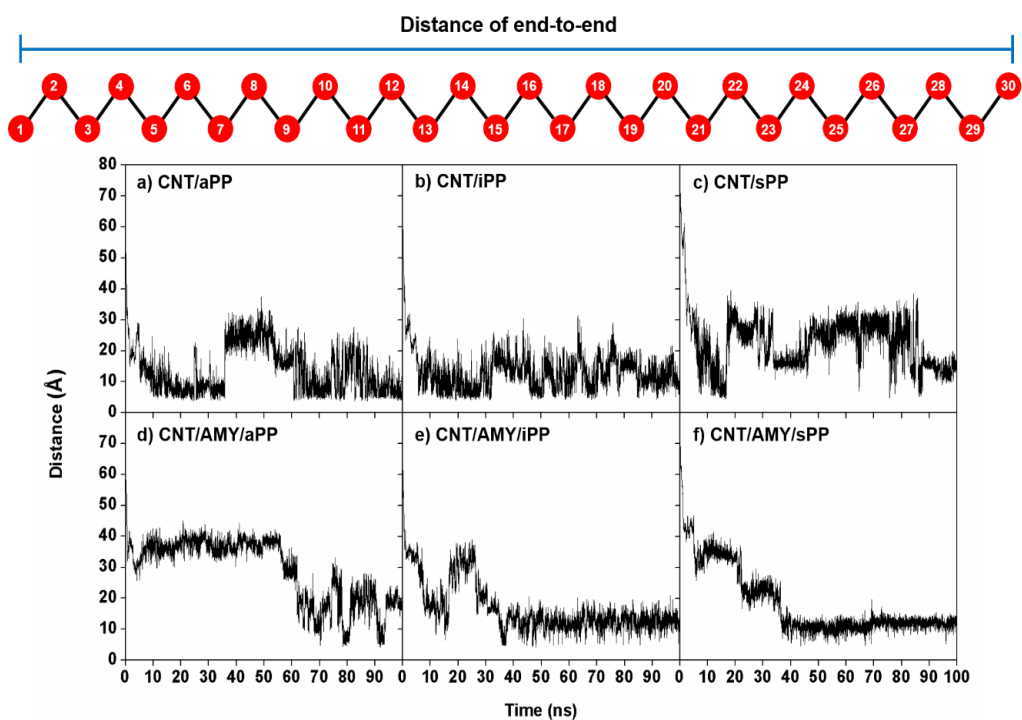
Figure 4.9 The distance of end-to-end chain of PPs for a) CNT/aPP, b) CNT/iPP, c) CNT/sPP, d) CNT/AMY/aPP, e) CNT/AMY/iPP and f) CNT/AMY/sPP systems calculated from the last MD snapshot in **Figure 4.3**.
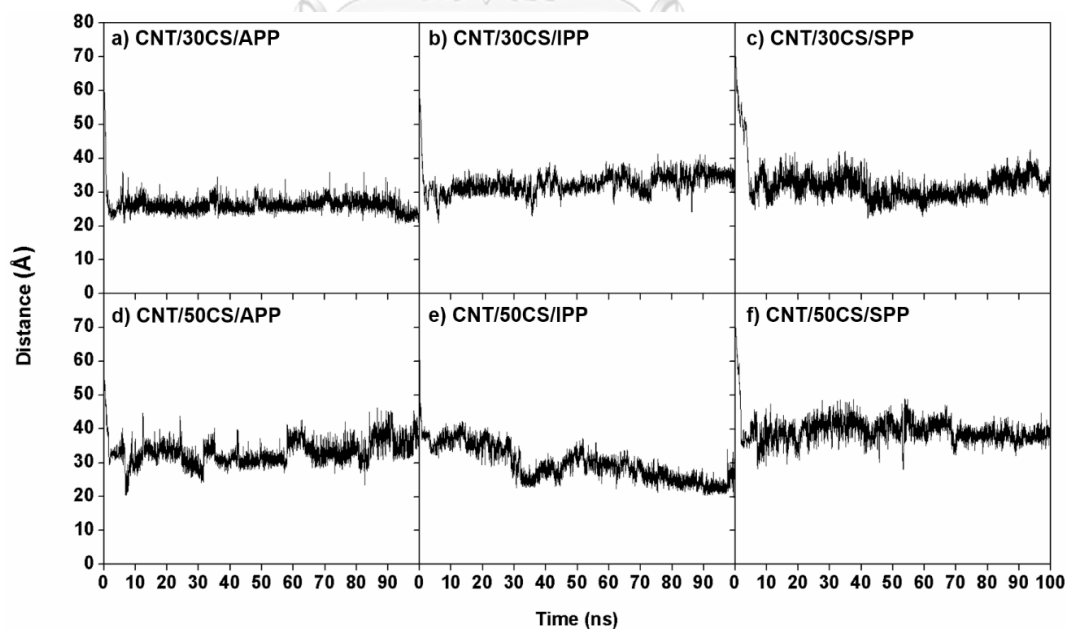
Figure 4.10 The distance of end-to-end chain of PPs for a) CNT/30CS/aPP, b) CNT/30CS/iPP, c) CNT/30CS/sPP, d) CNT/50CS/aPP, e) CNT/50CS/iPP and f) CNT/50/50CS/sPP systems calculated from the last MD snapshot in **Figure 4.4**.

4.6 **Electrostatic and van der Waals interactions energy**

- The CNT/PPs systems without and with AMY non-covalent modification CNT surface

The electrostatic (ΔE_{ele}) and van der Waals (ΔE_{vdW}) interaction energies between PP and CNT for the systems without and with AMY modification evaluated using the cpptraj module implemented in AMBER16 are given in **Figure 4.11**. Considering all systems without AMY wrapping, the ΔE_{ele} and ΔE_{vdW} values between PPs and CNT are ~2800 kcal/mol and ~-350 kcal/mol, respectively, suggesting that the vdW interaction is the main force for molecular complexation. Interestingly, in case of the systems with AMY non-covalently conjugated on CNT, both interaction energies of all PPs are dramatically reduced to ~-1500 and ~-800 kcal/mol for ΔE_{ele} and ΔE_{vdW}, respectively. From this analysis, it can be concluded that AMY wrapping could promote the binding efficacy of PPs toward CNT through both ele and vdW interactions in accordance with the previous works [20, 40-42]. For the ele interaction energy of PP with AMY and CNT (PP-AMY$^{(CNT/AMY)}$ and PP-CNT$^{(CNT/AMY)}$) for CNT/PPs (**Figure 4.12)**, it shows that the attractive and repulsive forces are found. In contrast, the vdW interaction of PP-CNT$^{(CNT/AMY)}$ is stronger than PP-AMY$^{(CNT/AMY)}$ by c.a. 100-150 kcal/mol.
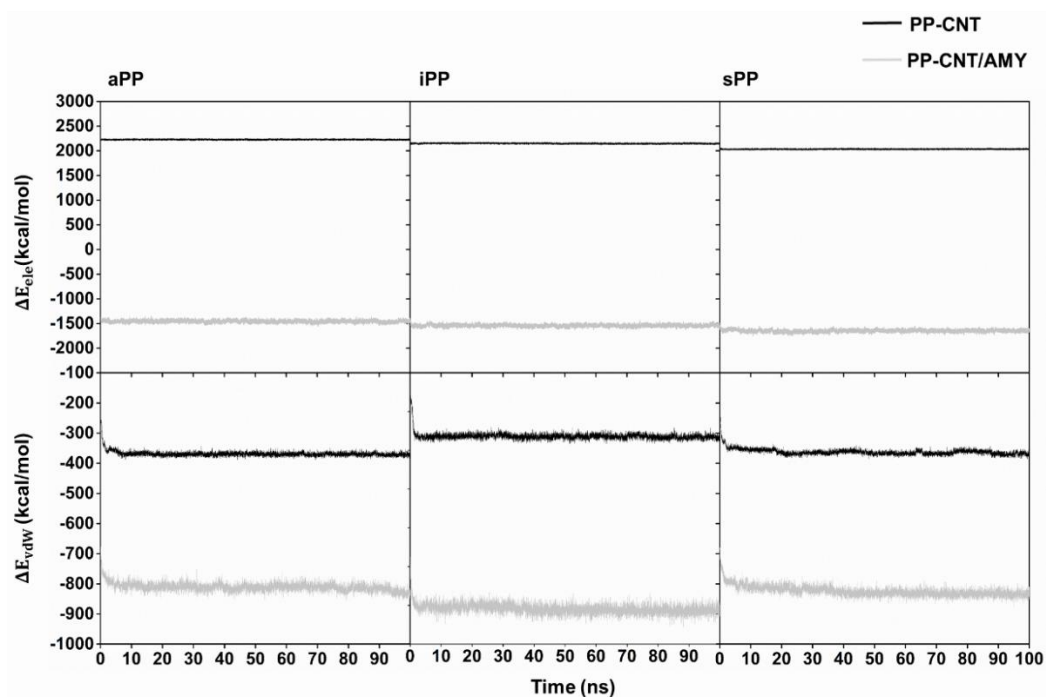
Figure 4.11 Electrostatic and van der Waals interaction energies (ΔE_{ele} and ΔE_{vdW}) between PP and CNT without (black) and with AMY modification (light grey).
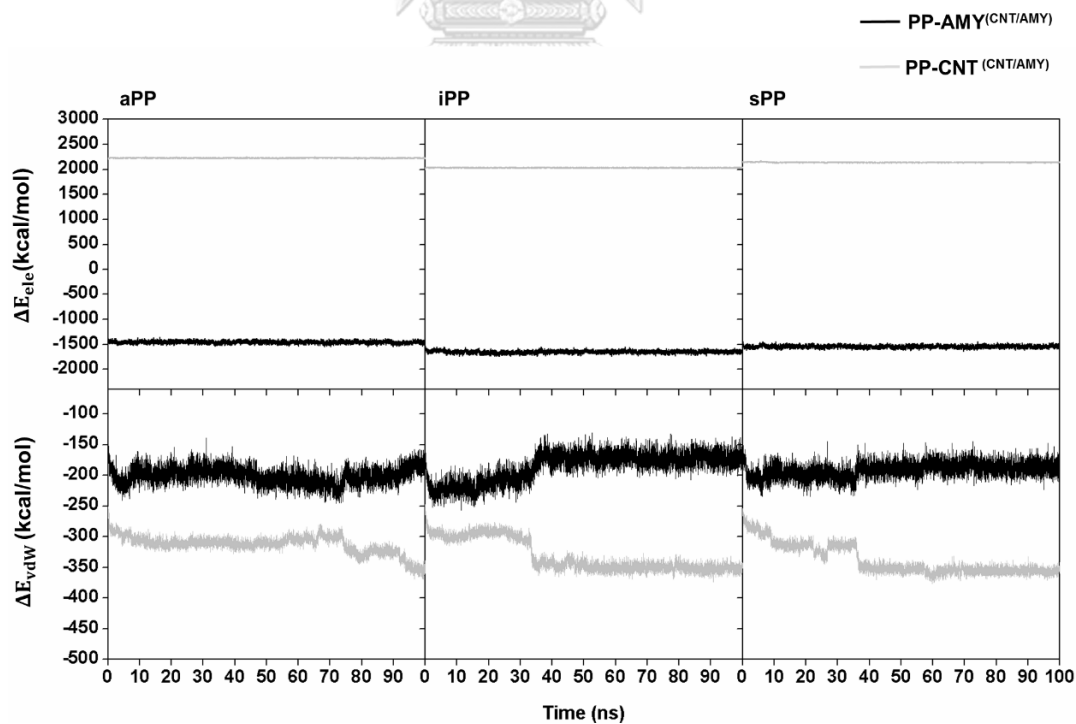
Figure 4.12 Electrostatic and van der Waals interaction energies (ΔE_{ele} and ΔE_{vdW}) between PP and AMY (PP-AMY$^{(CNT/AMY)}$, black) and CNT (PP-CNT$^{(CNT/AMY)}$, light grey) of the AMY modification system

- The CNT/PPs systems with different length CS non-covalent modification CNT surface

The ΔE_{ele} and ΔE_{vdW} interaction energies between PP and CNT for the systems with different length CS modification evaluated using the cpptraj module implemented in AMBER16 are given in **Figure 4.12**. Considering all systems with 30CS wrapping, the ΔE_{ele} and ΔE_{vdW} values between PPs and CNT/30CS of ~-1000 kcal/mol and ~-800 kcal/mol, respectively, suggesting that the ele interaction is the main force for molecular complexation. Interestingly, in case of the systems with 50CS non-covalently conjugated on CNT, both interaction energies of all PPs are dramatically reduced to ~-3000 and ~-1200 kcal/mol for ΔE_{ele} and ΔE_{vdW}, respectively. For the ele interaction energy of PP with 30CS and 50CS (PP-CS$^{(CNT/30CS)}$ and PP-CNT$^{(CNT/50CS)}$) for CNT/PPs (**Figure 4.13 and Figure 4.14**), it shows that the attractive forces are found and the ele interaction of PP-CS$^{(CNT/30CS)}$ and PP-CNT$^{(CNT/50CS)}$ are stronger than vdW interaction.

Figure 4.13 Electrostatic and van der Waals interaction energies (ΔE_{ele} and ΔE_{vdW}) between PP and CNT with 30 (black) and 50 CS repeating units modification (light grey).
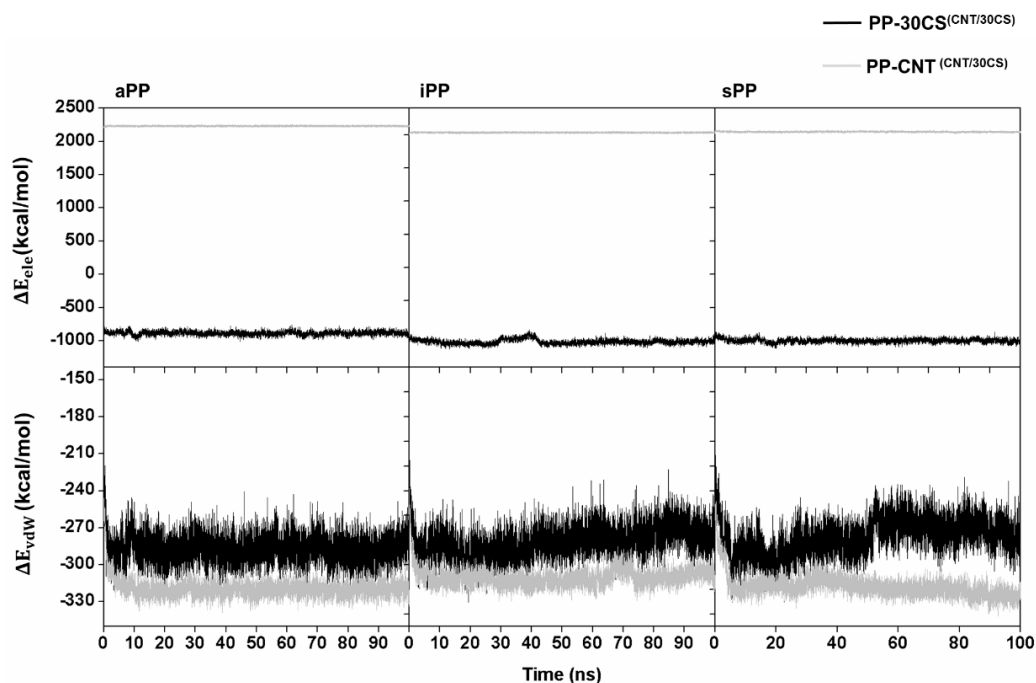
Figure 4.14 Electrostatic and van der Waals interaction energies (ΔE_{ele} and ΔE_{vdW}) between PP and 30CS (PP-30CS$^{(CNT/30CS)}$, black) and PP and CNT (PP-CNT$^{(CNT/30CS)}$, light grey) of the 30 units CS modification system

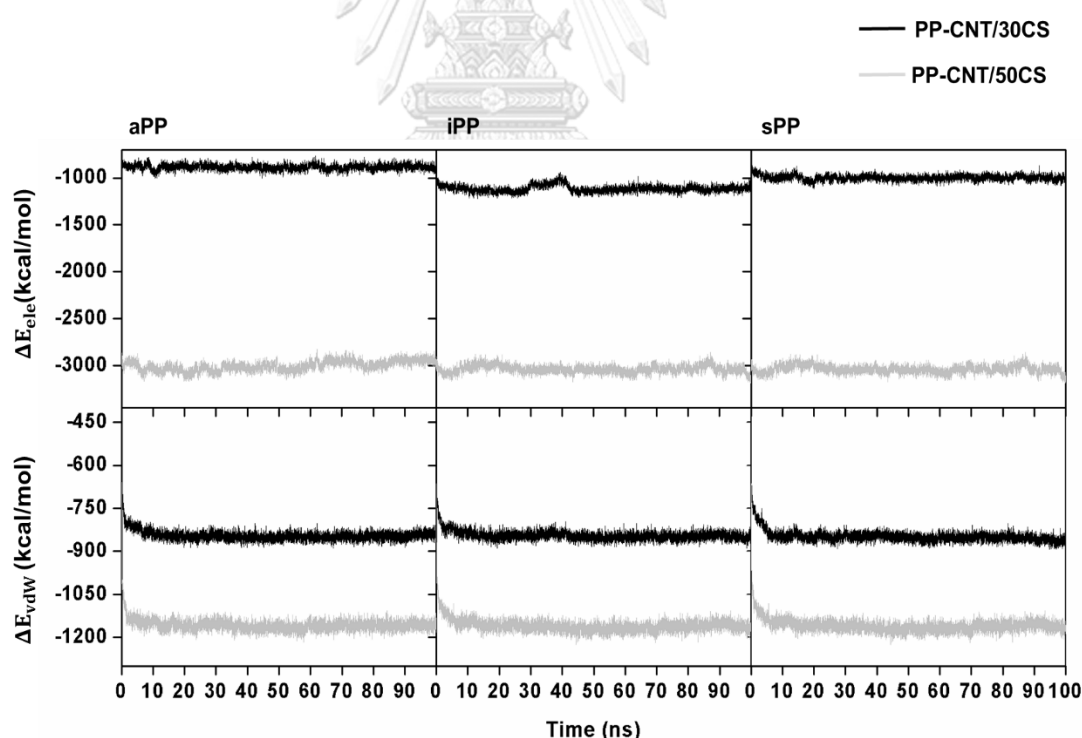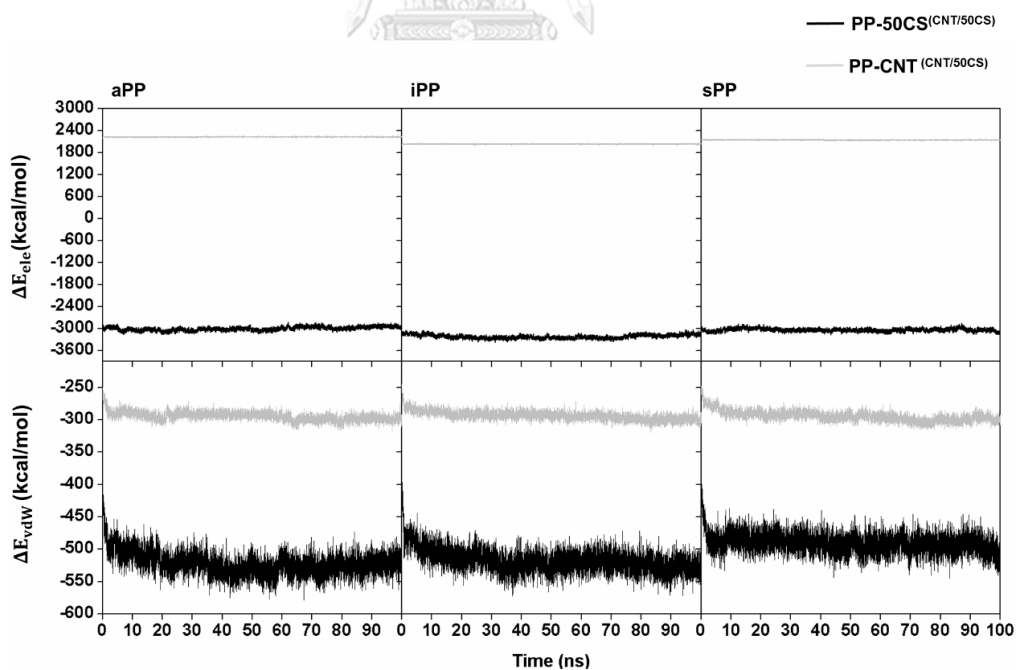**Figure 4.15** Electrostatic and van der Waals interaction energies (ΔE_{ele} and ΔE_{vdW}) between PP and 50CS (PP-50CS$^{(CNT/50CS)}$, black) and PP and CNT (PP-CNT$^{(CNT/50CS)}$, light grey) of the 50 units CS modification system

4.7   Conclusion

In the present study, the all-atom MD simulation for 100-ns reveals that AMY non-covalently modified on CNT outer surface could induce the PPs binding toward CNT with a formation of better-formed nanocomposite, especially for the iPP and sPP systems in the AMY modification. This structural transformation occurrs by a significant reduction of distance between the center of gravity of end-to-end of iPP and sPP. However, the aPP is not completely wrapped with CNT due to the high flexibility of its terminal chain. The radius of gyration results support that iPP and sPP could spirally wrap with CNT in a presence of AMY in a correspondence with the enhanced orderliness of angle distribution in between PP chain itself.

In case of CNT modified by CS, the binding of PPs on CNT is found inin snack-like manner, in which the distance of end-to-end of PP is higher than AMY systems and Rg of PP is higher than Rg CS. Moreover, the main interaction causing PPs to become spirally contacts with CNT/AMY is electrostatic attraction. Taken together, AMY and CS wrapped around CNT exterior could significantly increase the interfacial adhesion of PPs toward CNT, which can be used as a rational guide for the synthesis of PPs/CNT nanocomposites for further applications.

REFERENCES

1. Porter, D., E. Metcalfe, and M.J.K. Thomas, *Nanocomposite fire retardants — a review.* Fire and Materials, 2000. **24**(1): p. 45-52.

2. Aqel, A., et al., *Carbon nanotubes, science and technology part (I) structure, synthesis and characterisation.* Arabian Journal of Chemistry, 2012. **5**(1): p. 1-23.

3. Li, X.-H., et al., *Simultaneous Enhancements in Toughness and Electrical Conductivity of Polypropylene/Carbon Nanotube Nanocomposites by Incorporation of Electrically Inert Calcium Carbonate Nanoparticles.* Industrial & Engineering Chemistry Research, 2017. **56**(10): p. 2783-2788.

4. Rungrotmongkol, T., et al., *Increased dispersion and solubility of carbon nanotubes noncovalently modified by the polysaccharide biopolymer, chitosan: MD simulations.* Chemical Physics Letters, 2011. **507**(1): p. 134-137.

5. Rungnim, C., T. Rungrotmongkol, and R.P. Poo-arporn, *pH-controlled doxorubicin anticancer loading and release from carbon nanotube noncovalently modified by chitosan: MD simulations.* Journal of Molecular Graphics and Modelling, 2016. **70**(Supplement C): p. 70-76.

6. Tjong, S.C., *Structural and mechanical properties of polymer nanocomposites.* Materials Science and Engineering: R: Reports, 2006. **53**(3): p. 73-197.

7. Banerjee, S., T. Hemraj-Benny, and S.S. Wong, *Covalent Surface Chemistry of Single-Walled Carbon Nanotubes.* Advanced Materials, 2005. **17**(1): p. 17-29.

8. Li, C. and T.-W. Chou, *A structural mechanics approach for the analysis of carbon nanotubes.* International Journal of Solids and Structures, 2003. **40**(10): p. 2487-2499.

9. Spitalsky, Z., et al., *Carbon nanotube–polymer composites: Chemistry, processing, mechanical and electrical properties.* Progress in Polymer Science, 2010. **35**(3): p. 357-401.

10. Liu, Y. and S. Kumar, *Polymer/Carbon Nanotube Nano Composite Fibers–A Review.* ACS Applied Materials & Interfaces, 2014. **6**(9): p. 6069-6087.

11. Endo, M., M.S. Strano, and P.M. Ajayan, *Potential Applications of Carbon Nanotubes*, in *Carbon Nanotubes: Advanced Topics in the Synthesis, Structure, Properties and Applications*, A. Jorio, G. Dresselhaus, and M.S. Dresselhaus, Editors. 2008, Springer Berlin Heidelberg: Berlin, Heidelberg. p. 13-62.

12. Kashiwagi, T., et al., *Thermal and flammability properties of polypropylene/carbon nanotube nanocomposites.* Polymer, 2004. **45**(12): p. 4227-4239.

13. Rahmat, M. and P. Hubert, *Carbon nanotube–polymer interactions in nanocomposites: A review.* Composites Science and Technology, 2011. **72**(1): p. 72-84.

14. Papageorgiou, G.Z., et al., *Isotactic Polypropylene/Multi-Walled Carbon Nanotube Nanocomposites: The Effect of Modification of MWCNTs on Mechanical Properties and Melt Crystallization.* Macromolecular Chemistry and Physics, 2013. **214**(21): p. 2415-2431.

15. Tsuyohiko, F. and N. Naotoshi, *Non-covalent polymer wrapping of carbon nanotubes and the role of wrapped polymers as functional dispersants.* Science and Technology of Advanced Materials, 2015. **16**(2): p. 024802.

16. Beyer, G., *Nanocomposites: a new class of flame retardants for polymers.* Plastics, Additives and Compounding, 2002. **4**(10): p. 22-28.

17. Zhang, S. and A.R. Horrocks, *A review of flame retardant polypropylene fibres.* Progress in Polymer Science, 2003. **28**(11): p. 1517-1538.

18. Liang, J.Z. and R.K.Y. Li, *Rubber toughening in polypropylene: A review.* Journal of Applied Polymer Science, 2000. **77**(2): p. 409-417.

19. Deng, H., et al., *Effective reinforcement of carbon nanotubes in polypropylene matrices.* Journal of Applied Polymer Science, 2010. **118**(1): p. 30-41.

20. Tallury, S.S. and M.A. Pasquinelli, *Molecular Dynamics Simulations of Flexible Polymer Chains Wrapping Single-Walled Carbon Nanotubes.* The Journal of Physical Chemistry B, 2010. **114**(12): p. 4122-4129.

21. Cai, X., et al., *Evaluation of amylose used as a drug delivery carrier.* Carbohydrate Research, 2010. **345**(7): p. 922-928.

22. van der Maarel, M.J.E.C., et al., *Properties and applications of starch-converting enzymes of the α-amylase family.* Journal of Biotechnology, 2002. **94**(2): p. 137-155.

23. Stam, M.R., et al., *Dividing the large glycoside hydrolase family 13 into subfamilies: towards improved functional annotations of α-amylase-related proteins.* Protein Engineering, Design and Selection, 2006. **19**(12): p. 555-562.

24. Souza, P.M.d. and P.r.d.O.e. Magalhães, *Application of microbial ±-amylase in industry - A review.* Brazilian Journal of Microbiology, 2010. **41**: p. 850-861.

25. Zhang, X., L. Meng, and Q. Lu, *Cell Behaviors on Polysaccharide-Wrapped Single-Wall Carbon Nanotubes: A Quantitative Study of the Surface Properties of Biomimetic Nanofibrous Scaffolds.* ACS Nano, 2009. **3**(10): p. 3200-3206.

26. Xie, Y.H. and A.K. Soh, *Investigation of non-covalent association of single-walled carbon nanotube with amylose by molecular dynamics simulation.* Materials Letters, 2005. **59**(8): p. 971-975.

27. Aztatzi-Pluma, D., et al., *Study of the Molecular Interactions between Functionalized Carbon Nanotubes and Chitosan.* The Journal of Physical Chemistry C, 2016. **120**(4): p. 2371-2378.

28. Basu, D., C. Datta, and A. Banerjee, *Biodegradability, mechanical properties, melt flow index, and morphology of polypropylene/amylose/amylose-ester blends.* Journal of Applied Polymer Science, 2002. **85**(7): p. 1434-1442.

29. Salmah, H., F. Amri, and H. Kamarudin, *Properties of Chitosan-Filled Polypropylene (PP) Composites: The Effect of Acetic Acid.* Polymer-Plastics Technology and Engineering, 2012. **51**(1): p. 86-91.

30. Gunsteren, W.F.v. and H.J.C. Berendsen, *Computer Simulation of Molecular Dynamics: Methodology, Applications, and Perspectives in Chemistry.* Angewandte Chemie International Edition in English, 1990. **29**(9): p. 992-1023.

31.   Duan, Y., et al., *A point-charge force field for molecular mechanics simulations of proteins based on condensed-phase quantum mechanical calculations.* Journal of Computational Chemistry, 2003. **24**(16): p. 1999-2012.

32.   Kirschner, K.N., et al., *GLYCAM06: A generalizable biomolecular force field. Carbohydrates.* Journal of Computational Chemistry, 2008. **29**(4): p. 622-655.

33.   Wang, J., et al., *Development and testing of a general amber force field.* Journal of Computational Chemistry, 2004. **25**(9): p. 1157-1174.

34.   Ryckaert, J.-P., G. Ciccotti, and H.J.C. Berendsen, *Numerical integration of the cartesian equations of motion of a system with constraints: molecular dynamics of n-alkanes.* Journal of Computational Physics, 1977. **23**(3): p. 327-341.

35.   Darden, T., D. York, and L. Pedersen, *Particle mesh Ewald: An N·log(N) method for Ewald sums in large systems.* The Journal of Chemical Physics, 1993. **98**(12): p. 10089-10092.

36.   Roe, D.R. and T.E. Cheatham, *PTRAJ and CPPTRAJ: Software for Processing and Analysis of Molecular Dynamics Trajectory Data.* Journal of Chemical Theory and Computation, 2013. **9**(7): p. 3084-3095.

37.   Yang, S., S. Yu, and M. Cho, *Influence of Thrower–Stone–Wales defects on the interfacial properties of carbon nanotube/polypropylene composites by a molecular dynamics approach.* Carbon, 2013. **55**: p. 133-143.

38.   Liu, W., et al., *Interactions between Single-Walled Carbon Nanotubes and Polyethylene/Polypropylene/Polystyrene/Poly(phenylacetylene)/Poly(p-phenylenevinylene) Considering Repeat Unit Arrangements and*

Conformations: A Molecular Dynamics Simulation Study. The Journal of Physical Chemistry C, 2008. **112**(6): p. 1803-1811.

39. Grosberg, A.Y., P.G. Khalatur, and A.R. Khokhlov, *Polymeric coils with excluded volume in dilute solution: The invalidity of the model of impenetrable spheres and the influence of excluded volume on the rates of diffusion-controlled intermacromolecular reactions.* Die Makromolekulare Chemie, Rapid Communications, 1982. **3**(10): p. 709-713.

40. Yang, J., et al., *Morphology, thermal stability, and dynamic mechanical properties of atactic polypropylene/carbon nanotube composites.* Journal of Applied Polymer Science, 2005. **98**(3): p. 1087-1091.

41. Kearns, J.C. and R.L. Shambaugh, *Polypropylene fibers reinforced with carbon nanotubes.* Journal of Applied Polymer Science, 2002. **86**(8): p. 2079-2084.

42. Lee, S.H., et al., *Rheological and electrical properties of polypropylene composites containing functionalized multi-walled carbon nanotubes and compatibilizers.* Carbon, 2007. **45**(14): p. 2810-2822.

APPENDIX

Conferences (Poster presentation)

1. The 21st Annual Symposium on Computational Science and Engineering (ANSCSE21), Thailand Science Park, Pathum Thani, Thailand, August 3-4, 2017.

   Topic: Polypropylene and Amylose Wrapping on Single-wall Carbon Nanotube by Computational Study

2. The 43rd Congress on Science and Technology of Thailand (STT 43), Chulalongkorn University, Bangkok, Thailand, October 17-19, 2017.

   Topic: A Molecular Dynamics Study of Amylose/Polypropylene Non-Covalently Wrapped on Single-Wall Carbon Nanotube

3. The First Materials Research Society of Thailand International Conference (1st MRS Thailand International Conference), Convention Center, Empress Hotel, Chiang Mai, Thailand, October 31 - November 3 2017.

   Topic: Molecular Dynamics Study on Amylose and Polypropylene Wrapped on Single-Wall Carbon Nanotube

4. The 1st Taiwan-Thailand-Vietnam Workshop on Theoretical and Computational Chemistry, The National Taiwan University of Science and Technology, Taipei, Taiwan, March 22-23, 2018.

   Topic: A molecular dynamics study of amylose/polypropylene non-covalently wrapped on single-wall carbon nanotube

Publication

1. W. Panman, P. Mahalapbutr, O. Saengsawang, C. Rungnim, N. Kungwan, T. Rungrotmongkol[*], S. Hannongbua[*], "Conjugated amylose-assisted the binding of polypropylene toward single-walled carbon nanotube: A molecular dynamics simulation", Journal of Computational and Theoretical Chemistry, 2018, submitted

2. P. Wongpituk, B. Nutho, W. Panman, N. Kungwan, P. Wolschann, T. Rungrotmongkol[*], N. Nunthaboot[*], "Structural dynamics and binding free energy of neral-cyclodextrins inclusion complexes: molecular dynamics simulation", Molecular Simulation, (43)2017, 1356-1363.

3. W. Panman, B. Nutho, S. Chamni, S. Dokmaisrijan, N. Kungwan, T. Rungrotmongkol[*], "Computational screening of fatty acid synthase inhibitors against thioesterase domain", Journal of Biomolecular Structure and Dynamics, 2017, DOI: 10.1080/07391102.2017.1408496

4. W. Panman[#], P. Mahalapbutr[#], A. Opasmahakul, N. Kungwan, S. Hannongbua, T. Rungrotmongkol[*], "Atomistic mechanisms underlying the activation of G protein-coupled sweet receptor heterodimer mediated by sugar alcohol recognition: A molecular dynamics study", Scientific Reports, 2018, submitted

VITA

Personal data:

Name: Wanwisa Panman

Nationality: Thai

Date of birth: 14 July, 1992

Place of birth: Nakhon Si Thammarat, Thailand

E-mail address: mwwanwisa@gmail.com

Educations:

20011-2014 B.Sc. (Computational Chemistry), Walailak University, Thailand